POLITECNICO DI MILANO
DEPARTMENT OF MECHANICAL ENGINEERING
DOCTORAL PROGRAMME IN MECHANICAL ENGINEERING

INNOVATIVE TECHNIQUE TO ASSESS TENSILE AXIAL LOAD IN TIE-RODS BY MEANS OF DYNAMIC MEASUREMENTS

Doctoral Dissertation of:

Matteo Scaccabarozzi

Supervisor:
Prof. Alfredo Cigada

Tutor:
Prof. Stefano Bruni

The Chair of the Doctoral Program:
Prof. Bianca Colosimo

2014 – Cycle XXVII

Abstract

In many civil structures, both historical and modern kind, tie-rods, or tie-beams, represent a useful and common tool to balance the lateral force at the base of arches and vaults. A measurement of the tensile axial load hold by them is an important feature for an effective health monitoring of the whole structure where the beams are inserted in. This thesis deals with a new method to estimate axial load in tie-rods by means of indirect measurements.

The state of the art about the topic is largely oriented to employ dynamic measurements, because of advantages of an easier experimental set up then those required by static methods. However, the dynamic behaviour of a tie-rod is affected by few parameters, not only by the axial load, e.g. the boundary conditions as well as the geometrical and material property of the beam. Only a few of them can be evaluated with accuracy. In literature, only a few studies taken into account the uncertainties on parameters such as the actual free length of the tie-rods as well as the physical properties of the material which constitutes the beam. Moreover, most of methods rely on the solution of analytical model consistent only with constant cross-section beams.

The innovative method proposed relies on the experimental estimation of the tie-rod eigenfrequencies and mode shapes in a limited number of points. Furthermore, the approach requires to develop a simple finite element model, which is then cross-correlated with the experimental data by means of a model updating procedure. The effect of uncertainties on the aforementioned parameters is investigate in depth. The work aims to provide a reliable evaluation of the constraints behaviour by means of the mode shapes components measured in one/two points. In order to do that, two different ways as developed and compared. One of them works either measuring or not the input to the tie-rod. A set of eigenfrequencies are identified in order to provide a first evaluation of the axial load and then the modal updating procedure is performed to achieve a set of final value for each parameter.

Extensive numerical simulations and experimental tests demonstrated the capability of the new approach to give accurate estimates of the tie-rod axial load, also accounting for the aforementioned uncertainties. The method overcome some limitations of the methods currently available in literature. Furthermore, the algorithm can work either measuring or not the input to the tie-rod. The possibility to use operational modal analysis allows to implement a continuous monitoring of the tie-rod axial load.

Summary

List of Figures

CHAPTER 1

Introduction and state of the art

1.1 Introduction

In architectural tradition, the insertion of metallic tie-rods, or tie-beams, in masonry structures is a commonly and reliable solution in order to balance the lateral force at the base of arches and vaults. In Italy, a lot of the historical buildings bear witness to the use of such structural elements since the 13th century. Thereafter, tie-rod application remained the usual procedure up to the advent of steel and reinforced concrete buildings, and much of European architectural heritage testifies to its widespread use. Moreover, the consolidation works carried out on a lot of historical buildings has led to insert tie-rods also where they are not originally placed, in order to help masonry structures in bearing the lateral loads.

It was a standard practice to provide a pre-tensile load to the tie-rods when they are placed in the structure. Usually, the beam is heated to yield its thermal elongation. Then, after that the beam ends are constrained, the tensile axial load increases as soon as the tie-rod cools. Without carrying out a measurement of the load during the pre-tension operation, e.g. by means of a strain gauge, then it is impossible to provide a direct measurement of the absolute load. However, because of the critical role that tie-rods play in the stability of many historical buildings, it is useful to have a reliable methodology that enables non-destructive assessment of the pull tension on already operant tie-rods. Due to settlements of the structural ensemble where the tie-rods are placed, their tensile force can change. An overload applied on one of them could cause

the tie-rod to exceed the maximum elastic stress of the beam material. This state could yield to displacement larger than those bearable by the static balance of the structure itself. Moreover, the beam might not support any increase in load or, in a worst-case scenario, it could suffer a mechanical failure. This could be particularly dangerous in the event of any exceptional environmental forcing situations such as earthquakes. Giuriani et al. [1] proposed a simplified analytical model concerning the seismic vulnerability of arches, which estimated both tie over-tension and the collapse multiplier in transverse arch rocking condition. In particular, the seismic assessment of the transverse arch vulnerability has to be referred to both the tie yielding and the tie anchorage failure. Aimed at preserving the tie-rod in elastic range and limiting the overall displacement of the transverse arch rocking mechanism, an accurate evaluation of the axial force in the tie rod is an important goal. Conversely, due to any constraint yielding, the work of a tie-rod may become ineffective in ensuring structural equilibrium (i.e. tension is lower than that predicted at the design stage). This would yield subsidence in the static attitude of the whole structure. Moreover, in ancient or historical buildings, chemical corrosion can play a role in decreasing the strength of tie-rods, and this may lead to a redistribution of the loads among all the tie-rods in the structure. In any case, monitoring the evolution in time of a tie-rod tensile force could provide timely warning of any change in the overall structural health. Furthermore, when a restoration work is to be carried out on historical building in which tie-rods are present, sometimes it is necessary to replace some of them. Also in this case, it is indispensable to know the actual stress state of the rod, in order to arrange any temporary element capable of ensuring the balance of lateral load provided by the rod which will be removed.

The only way to have an accurate measurement of the axial load may be to bond strain gauges or fix a load cell on the beam before tensing it. Obviously, this requirement is impossible to have on the ancient tie-rods of a historical building or in all previously installed tie rods. It may be a critical task also in more modern building, where tie-rods are employed. Without this condition, there is no non-destructive technique for direct in-situ measurement of the tensile force on the beam. So far, different methods have already been proposed in order to assess an indirect measurement of the axial load on slender beam. Some of them are based on static measurements [2, 3, 4], others rely on dynamic type [5, 6, 3, 7, 8, 9, 10, 11, 12], still others use both kinds [13, 14]. In any case the axial force is not the only unknown variable. In real cases, also the parameters characterizing the constraints and the material specifications are almost unknown, especially when historical sites are considered. Several techniques concerning the

assessment of the axial stress in a beam have been generalized by taking into account both of tensile and compressive load. This approach aims to be suitable not only for the tie-rods at the base of arches and vaults but also for the struts and ties of a space truss structure, or the diagonal braces of a truss girder as well. However, the development of an experimental technique which should be reliable in the specific assessment of the axial load on an ancient tie-rod is a target that should take into account some particular conditions. For example, in many cases the tie-rods in historical buildings are placed in site not easily accessible, as Fig. 1-1 shows.

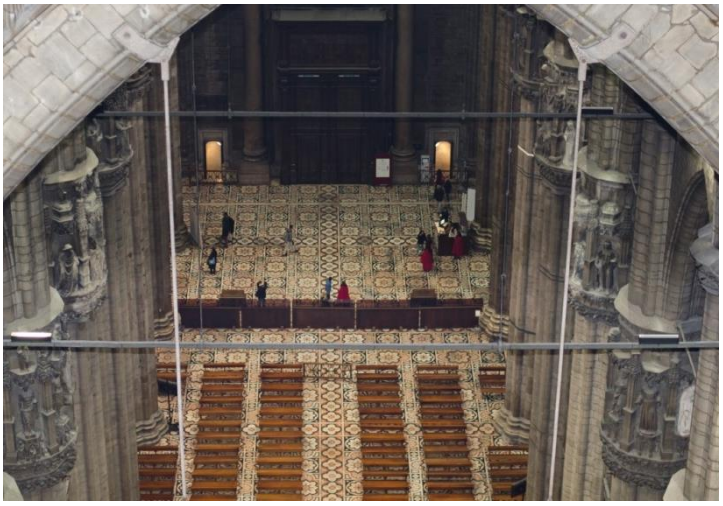

Fig. 1-1: tie-rods in the nave of Duomo in Milan

Normally, the boundary conditions at the ends of the beams are not completely known or it is not easy to model their behaviour, as Fig. 1-2 and Fig. 1-3 can suggest.

The last figure also highlights how many ancient tie-rods could show a deterioration of the material such as to cause a non-uniform cross section along the beam. Some of them may present a non-monolithic layout, such as the rod show in Fig. 1-5, which is composed by mean of multi-layer sheets. In some cases, tie-rods may support one or more added masses, as it is shown in Fig. 1-4. In many cases tie-rods are composed by two beams, which are joined and tight by means of a screwed coupling joint, which means to have a non-uniform mass-for-unit-length distribution and a local change in flexural stiffness as well [8].

Fig. 1-2: tie-rods in Visso (MC) - Italy

Fig. 1-3: tie-rods in Recanati (MC) - Italy

All these issues suggest that a method based on the solution of a purely analytical model by means of inputs measured on a real tie-rod may show some limits, due to the simplified hypothesis request by the analytical approach available (i.e. Euler-Bernoulli beam theory). That approach yields good results in case of rods with characteristics very close to those requested by the model, but obviously could lead to biased results in case of not ideal conditions.

Fig. 1-4: tie-rod with added mass in Loreto's Basilica (AN) - Italy

Fig. 1-5: multi-layer tie-rod in Loreto's Basilica (AN) - Italy

A technique based on finite element model (FEM) could provide the suitable flexibility in order to take into account particular configuration of the structure. Finite element formulations coupled with model updating techniques can lead to the goal. In [15, 16, 17] vibration response of the entire structure are used in order to identify the axial force of all frame elements, but the accuracy, even the reliability, strongly depends on the uncertainty of the FE model, as Rebecchi et al. [11] suggested. Amabili et al. [7]

proposed a technique that employs dynamic measurement, a Timoschenko beam model and a minimization procedure in order to assess the axial load in tie-rod. Gentilini et al. [9] prefer to employ genetic algorithms aiming to achieve results minimally affected by the initial guess of the target variables. In principle, to develop a FE model of the tie-rod which is object of the investigation can be a good way for achieve a technique working with different lay out of rod.

Other significant issue should be taken into account in undertaking the development of a method aiming to the discussed question, i.e. the nature of the experimental technique requested by procedure. Since tie-rods are often placed at considerable heights and may have a remarkable span, the more easier and faster the measuring procedure are the more cost effective the method is. These issues leaded many works oriented to dynamic measurements, instead of the static kind. In addition, another important feature which is investigable in dynamic based method is the capability of the method to work also exploiting the environmental forcing. This opportunity can yield significant advantages in ensuring a effective structural health monitoring.

Describing in more detail the state of the art present in literature, the techniques are divided according to the king of measurements that they employ, i.e. static or dynamic measurements.

1.2 Static methods

Briccoli Bati and Tonietti [2] introduced a technique based on a merely static identification. This method shows several advantages, e.g. the constraint conditions and Young's modulus need not to be known and also the processing of the resulting experiment data is quite simple. In fact, the entire problem reduces to solving a system of three linear equations with three unknowns, by means of experimental data which are achieved by three points of measurements: two of them close to the rod ends and the other in the middle. In this positions the bending moment must be measured by means of strain gauges and the vertical displacements due to a transverse load applied are needed as well. Blasi and Sorace [13] raise the question about the poor reliability of measurement obtained through strain gauge applied in proximity of the tie-rod end sections, because of presumed bond effects. Briccoli Bati and Tonietti reply that there is no reason to limit the transverse load to be applied as consequent increase in the

tension value is modest. This arrangement would produce a higher value of bending moment at the rod ends, so the measurement would be less affected by uncertainty. However, the risk to yield an overload an ancient tie-rod makes it advisable to not overdo with the transverse load, in order to avoid any permanent damage on the structure. Experimental validation of the technique was undertaken, showing good results in terms of low percentage error between evaluated and measured axial force.

Lately, alternative static measurement methods were present by Tullini et al. [3] and Tullini [4]. Both works follow a similar approach. In particular the reference model is constituted by a prismatic beam of length L, which is subjected to an axial force N and to a concentrate lateral load introduced by means of an added mass. Young's modulus E and cross-section area moment J are assumed to be known constants. Making use of the nondimensional coordinate z=x/L and neglecting both the shear deformations and rotary inertia, lateral displacement $v(z)$ is ruled by the following governing equation (Timoshenko and Gere [18], Meirovitch [19]):

$$EJ\frac{\partial^4 v(z,t)}{\partial x^4} + N\frac{\partial^2 v(z,t)}{\partial x^2} = 0 \tag{1}$$

The model used by Tullini et al. is a beam constrained by two end elastic-springs having flexural stiffness denoted by k_0 and k_1. This method needs the flexural displacements to be measured at three given cross sections in a bending test. According to this approach, the axial force as well as the flexural stiffness coefficient of the end constraints can be identified if the beam ends have infinite translation stiffness. So the procedure holds under condition that no displacement of the beam ends occurs. This is a quite restrictive assumption, as Tullini himself underlines in further work [4]. By means of experimental validations, taking into account a range of uncertainties in the flexural rigidity, the achieved results of the technique show that good agreement is obtained between estimated and measured values of the axial force, with percentage error equal or less than 10% for moderate or high value of tensile load. Conversely, the error rises for lower values of force, practically, the circumstances where static bending amplitude of the beam is more affected by the value of the constraints stiffness. In fact, the method is proving to be not very reliable to identify the flexural stiffness of the end constraints.

Tullini proposed a more recently identification method [4] which generalizes the algorithm earlier described, in order to study the more general problem of a prismatic slender beam with unknown boundary conditions. Tie-rods extremities are generally

embedded in masonry walls making doubtful the beam length and the locations of the end constraints. To overcome this problem, the method adopts a substructure of assigned length L, composed by a prismatic beam with uniform cross sections, constrained by means of two sets of elastic ends which allow the later displacements and rotations. The constraint parameters are $k_{\varphi\varphi}^{(i)}$, $k_{\nu\varphi}^{(i)}$, $k_{\nu\nu}^{(i)}$, $(i = 0, 1)$, which are collected by the $2x2$ stiffness matrices K_0 and K_1 (Fig. 1-6).

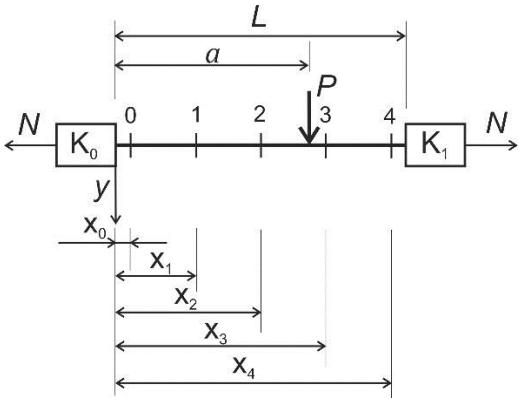

Fig. 1-6: beam model and measurement position in Tullini's method

This upgrade needs to arrange five points where measure displacement or bending curvature along the beam which is subjected to a concentrate lateral load.

The procedure is based on equation (1), which is solved by subdividing the beam into two intervals having length a and $L - a$, respectively. Then, the solutions v_I and v_{II} take form:

$$v_I(z) = C_1 cosh\sqrt{n}z + C_2 cosh\sqrt{n}z + C_3 z + C_4 \quad \text{for} \quad 0 < z < \alpha \tag{2a}$$

$$v_{II}(z) = C_5 cosh\sqrt{n}z + C_6 cosh\sqrt{n}z + C_7 z + C_8 \quad \text{for} \quad \alpha < z < 1 \tag{2b}$$

where $\alpha = a/L$ and $n = NL^2/EJ$ is the nondimensional axial force.

Five vertical displacements v_0, v_1, v_2, v_3, v_4 are measured after the application of a lateral load P. Functions (2a) are arranged in order to impose the five vertical displacement v_0, v_1, v_2, v_3, v_4. Hence, a system of eight linear functions makes coefficient $C_1, \dots, C_8$ dependent on the five experimental displacements v_0, v_1, v_2, v_3, v_4, the lateral load P and the unknown n. By imposing the internal conditions of the system, a transcendental equation is achieved and solved for the unknown constant n. Irrespective of the boundary condition, the solutions leads to the non-dimensional axial force. Provided that the Young's modulus is known, the technique can evaluate the

axial force value. After arranging in a suitable way the analytical system, same results are achievable also making use of strain sensors.

The technique was both numerically and experimentally validated, providing good results in term of tensile load as the previous work, but inaccurate estimates of the geometric and elastic material properties may influence the accuracy of the force identification. Tullini suggested that these effects might be reduced by increasing the number of sensors. A single model of simply supported beam was numerically studied in order to investigate how a scattered value of Young's modulus may affect the estimate axial force. The results are reassuring but the study has not been generalized. Besides this, even if the data-processing is quite straightforward, this method is extremely sensitive to the experimental uncertainties. In addition, since tie-rods are usually positioned at considerable heights, the need of measuring vertical deflections with respect to reference fixed base or using strain sensors (i.e. to solder a set of strain gauge on the rod, moving across at the top of a nave) makes methods difficult in practice.

1.3 Hybrid methods

Sorace [14] advanced an hybrid technique, using static as well as dynamic measurements, which enables to indirectly solve a system consisting of a static equation, giving the central deflection of the beam after applying a load, and a dynamic equation, giving the first vibration frequencies of the rod. Some problems may arise in the need to set up two different in-situ measurements. Tie-rod is modelled as constant cross-section beam whose restraints are schematized as two elastic rotational springs. Blasi and Sorace [13] have already presented an analytical closed-form relation between that model response and two parameters. Sorace generalized the method by means of a three-parameter model which takes into account different springs stiffness, by recording also the second vibration frequency. An analytical relation useful to estimate the Young's modulus is proposed, by measuring the middle-section bending moment. Finally, the axial load is estimated only after an analytical identification of the constraints stiffness. The strict dependence of the axial load to the constraint stiffness may easily leads to incorrect results due to uncertainties on the identification of the other parameters (i.e. the Young's modulus). The method does not take into account any uncertainty on the actual not constrained length of beam. An experimental

validation of the method was performed, providing differences between analytical estimates and experimental results slightly greater than 10%.

1.4 Dynamic methods

Focusing on the fully dynamic techniques, until a few years ago, the axial stress was evaluated by considering the tie-rod as a vibrating wire and measuring its first natural frequency. The advantage in considering these methods is to have a closed-form expression to solve the problem. However, they generally underrate the tensile force not taking into account the bending stiffness of the beam and of the constraints. Due to the correspondence with many practical situations, methods which involve bending stiffness effects have attracted extensive attention in recent years.

Lagomarsino and Calderini [6] present a method to assess the tensile axial load of tie-rods by identifying the first three natural frequencies of the structure. Tie-rods are easily excitable structures, whose modal frequencies can be easily identified through spectral analysis. Based on these considerations, the method relies on the minimization of an error function which takes into account three rod's eigenfrequencies. The tie-rod is assumed to be a beam, with uniform section. The density and the Young's modulus of the material are considered as data of the problem. The beam's length is assumed measurable on site with reasonable accuracy. However this assumption is effective if the constraints have not finite dimensions and are placed exactly where the tie-rod joints the walls. Boundary conditions neglect any transversal displacement on the beam ends. These conditions required by the method are rather restrictive moving to most of real cases.

The method introduced by Tullini and Laudiero [3] aims to identify the beam axial load by means of one vibration frequency and three component of the corresponding mode shape. The technique is based on Euler-Bernoulli's beam model, whose free-vibration equation of motion is (using the non-dimensional coordinate system $z = x/L$):

$$EJ\frac{\partial^4 v(z,t)}{\partial x^4} - NL^2\frac{\partial^2 v(z,t)}{\partial x^2} + \rho AL^4\frac{\partial^2 v(z,t)}{\partial t^2} = 0 \tag{3}$$

where $v(z,t)$ is the transverse-displacement response varying with position x and time t. The Young's modulus E, the density ρ, the cross-section area A and the cross-section

area moment of inertia J are assumed to beconstant, and known as well. The axial load is calculated by means of the analytical solution of the equation (3) on a reference model, which is constituted by a simply supported prismatic beam of length L, constrained at the ends by two end elastic-springs, whose stiffness is obtained by the method as well. The technique was experimentally validated providing good accuracy in identifying the axial load of the test rig. It should be stated that the Young's modulus and the density of the beam were experimentally evaluated, which is an hard task in almost any real case. Moreover, results in terms of elastic parameters (e.g. the constrain stiffness) are not always satisfactory. This work does not take into account any possible transverse displacement in correspondence with the visible ends of the tie-rod, neglecting any uncertainty on the actual free span of the beam as well.

The same authors and Rebecchi [11] generalized the above described method by studying the more general problem of a prismatic slender beam with unknown boundary conditions. The measurements of the mode shape components are undertaken on five positions distributed in an interval which is included in the span between the constraints of the beam: two at the interval extremities, two at the quarter sections and one at midspan. Also this extended method relies on accurate values of Young's modulus and density of a beam with constant cross-section. The experimental validation of the technique shows good results in terms of axial load identification. However, the method proves to be rather sensitive to the choice of the of the mode shape taken into account. The axial load is calculated by means of the solution of a transcendental equation dependent on bending moment of the beam (e.g. the Young's modulus and the cross-section), the density of the material, one eigenfrequency and a set of five corresponding mode shape amplitudes. By neglecting uncertainties of the material properties, the choice of where evaluating the mode shape amplitude may affected the accuracy of measurements. By trying to measure the mode shape component close to a node of that mode leads to lack of accuracy. Fox example, by taking into account the second mode shape of a beam, symmetrically constrained at the ends, it makes an hard task to perform an accurate measurement of the amplitude at the mid span. Finally, the method is able to give the axial load irrespective of boundary conditions but the constraints behaviour significantly affect the mode shapes and then the effectiveness in the choice of the position where measure their components. Experimental estimation of axial load shows a good matching with the measured tensile force according to the choice of the most appropriate mode shape, then a deeper investigation is need about this issue (i.e. in many real cases, the

dynamic properties of first mode shape is affected by the static flexural deformation of the tie-rod [20]).

Garziera et al. [8] propose a method which shows the advantage of being adaptable to many different tie-rid layout. Moreover, it takes into account uncertainties about constraints behavior and the actual free length of the beam. The technique relies on the identification of a set of natural frequencies, whose number is greater than the unknowns. A suitable optimisation algorithm is performed in order to achieve the best match between the experimental results and the frequencies obtained by a finite element model. As the numerical model allows analysis of very complicated problems, the method easily take into account also added masses or variable cross-section in the beam. This possibility allows to generalize the axial load identification also to tie-rods built into two separate chunks connected by means of a screwed coupling joint. This represent a very common solution for many rods with circular cross-section (see Fig. 1-7). The value of the added mass as well as the geometrical properties (i.e. the length) of the joint can be considered additional unknowns of the problem. The method relies on the optimization of an over-constrained problem, so the number of frequencies under investigation must overcome the number of unknowns. However, the accuracy in eigenfrequency identification becomes lower as soon as higher modes are taken into account. This issue limits the number of unknowns accounted in the analysis. So, the method was tested on a real application where uncertainties on the material properties are neglected. Unfortunatly, no direct measurements on the actual tensile force acting on the tie-rods were available. Any experimental testing for validation was not provide as well. So there is no checks on the effectiveness of the method.

Fig. 1-7: example of circular cross-section tie-rod with screwed coupling joint

A technique based on genetic algorithms is developed by Gentilini et al. [9]. The work aims to propose a procedure able to assess the axial load in a tie-rod, irrespective to initial values assumed for the structural parameters, able to identify the Young's modulus and both the different stiffness of the constraints as well. The tie-rod is still modeled as a uniform Euler-Bernoulli beam restrained at the ends by means of linear rotational springs. The unknowns are evaluated via an objective function designed as discrepancy between the experimental and numerical natural frequencies. Because of a non-symmetric stiffness of the constraints leads to a natural frequencies variation, the method investigates the frequencies of one/some modified systems obtained from the original tie-rod by adding a concentrated mass in a non-symmetric position. The position and the value of the concentrated mass affect the mode shape of the beam. In order to perform a reliable frequency identification, optimal locations of the forcing point as well as for accelerometers have to be determinate. To this purpose, a finite element model of the tie-rod under investigation is used to assess the intervals where the node of each accounted mode shape are included, according to a reasonable range of change in the unknown parameters. However, the method neglects any uncertainties about the actual free length of the tie-rod. The technique was numerically tested but no experimental validation was performed. Anyway, it has been applied to a real case. The required experimental equipment is not more cumbersome than that any other typical dynamic test, but the procedure appears rather time expensive, because of the repeated measurements for different positioning of the mass and impact points as well.

Li, et al. [10] take into account the first Tullini's work [3] aiming to overcome any lack of accuracy in results due to uncertainties on the effective vibration length of the beam as well as the hypothesis of infinite translational stiffness at the ends. More or less in parallel with Tullini, the two groups of authors developed similar extensions of the aforementioned approach.

Maes et al. [12] proposed a deeper investigation accounting for the shear deformation and the rotation inertia of the bar, e.g. the analytical solution of the method relies on Timoshenko beam theory. The transversal force and moment equilibrium for a free beam section is described by means of:

$$\frac{\partial V(x,t)}{\partial x} + N\frac{\partial^2 v(z,t)}{\partial x^2} = \rho A\frac{\partial^2 v(z,t)}{\partial t^2} \tag{4}$$

$$S(x,t) + \frac{\partial M(x,t)}{\partial x} = \rho J \frac{\partial^2 \gamma(x,t)}{\partial t^2} \quad (5)$$

Where the shear force $S(x,t)$ and the bending moment $M(x,t)$ are both defined along the deformed beam coordinate system. $\gamma(x,t)$ is the rotation of the beam cross-section. The cross section A (accounted in equation (3)), geometric moment of inertia J, and material density ρ are assumed to be known. The method also takes into account the inertia of the measurement equipment. The work follows two approaches: a modal approach (e.g. the one proposed by [3], [10], [11]) and an innovative direct frequency domain approach. In the latter, the transvers displacement of the centreline $\hat{v}(x)$ is evaluated as the bar response due to harmonic loading at a single frequency ω, e.g. the operational deflection shape of the beam at that frequency [21]. Without loss of generality, $\hat{v}(x)$ can also be represent the Fourier transform of the bar response $v(x,t)$ due to broadband excitation. A great advantage of this approach is the fact that it does not require an intermediate modal parameter estimation step. Both approaches are numerically tested also performing an error analysis in order to take into account any uncertainties on the parameters: the geometric and material properties, the sensor properties as well as the distance between them. it is noticed that the worst case scenario accounts for only 0.1% of uncertainty for the geometric and material properties. The results achieved by means of the modal approach showed that not all modes accounted for estimating the axial load provide reasonable identifications. In case of a particular mode, whose modal displacement in correspondence with a sensor location becomes small compared the others, the corresponding axial force estimate become sensitive to small errors on the input parameters. There is no direct criterion which indicates for which of the modes an accurate estimate of the axial force is obtained. This can be seen as a general drawback of the modal characteristics approach. On the contrary, the work showed that the frequency domain approach generally yields slightly better results. However, this approach showed to become more sensitive to uncertainties on the input parameters as soon as the number of sensors is decreased. The experimental validation of the frequency domain approach was performed employing 14 accelerometers yielding accurate results. Tests with 5 accelerometers show to severely underestimate the axial load, especially for relatively low force values.

Although there are different methods in literature about the assessment of axial tensile force in tie-rods, each of them has some limits. One of the most important is that most

methods require very accurate estimates of the mechanical properties of the beam (e.g. Young's modulus, density) under investigation but this is seldom possible, especially when ancient structures are considered.

The aim of the present work is to design, develop and validate an innovative technique based on dynamic measurements and able to overcome most of the problems and limitations of the previous approaches. Particularly, the method is expected to be simple to apply (both experimentally and numerically), give accurate assessment of tensile force and be able to properly work with different kinds of tie-rods (e.g. with both uniform and non-uniform beam cross-sections). Furthermore, the method should not need any accurate estimation of material data. Actually, it should work properly even with rough nominal data. In addition, the new technique is expected to work even with operational modal analysis in order to apply an effective continuous monitoring of tie-rods.

This work proposes an experimental-numerical technique developed to identify the tensile force acting in tie-rods. This method requires to identify experimentally the first eigenfrequencies of the structure and the associated modal shape components in few beam points as well. These data, coupled to the development of a Finite Element (FE) model of the beam, allow to give a first approximate assessment of the axial load and the boundary conditions. Then, these estimates constitute the inputs to the FE model, which undergoes an updating procedure. The final output of such an algorithm is a refined axial load estimation.

One of the advantages of the technique proposed is to be usable with any kind of rod layout (e.g. non-uniform cross-section, presence of screwed coupling joints which are typical in tie-rods to apply load). Furthermore, the experimental set-up is easy and fast to implement, making the testing procedure suitable to apply to many tie-rods in a short time. Besides, the method proved to be usable with both experimental and operational modal analysis techniques. The method was tested both numerically and experimentally and the test set-up chosen was representative of a real installation.

CHAPTER 2

Modal behaviour of tie-rods

2.1 Introduction

The chapter aims to show how modal parameters of tie-rods are affected by axial force and other variables, so that possible strategies to estimate the tensile force can be drawn up. Among all parameters that affects the tie-rod dynamic behaviour, there are some which are measurable and therefore considered as known (e.g. geometry) and others that are unknown (e.g. tensile load, material properties). In this case, tensile load is the object of the analysis. Conversely, the other variables are considered as disturbances, whose effect on the rod dynamics has to be investigated to achieve the best possible accuracy in the axial force estimation. An initial guess on some of such variables is possible with an acceptable accuracy, while not for others. Therefore, the first point to discuss is to define which mechanical and geometrical parameters must be accounted for to estimate the axial load.

2.2 Transverse vibration of beams

A rigorous mathematical model widely used for describing the transverse vibration of beams is based on the TBT (or thick beam theory) [18] developed by Timoshenko in the 1920s. This model is more accurate in predicting the beam's response than the Euler-

Bernoulli beam theory (EBBT) [19]. Indeed, it has been shown in the literature that the predictions of the thick beam model are in excellent agreement with the results obtained from the exact elasticity equations and experimental results [22]. Historically, the first important beam model was the one based on the EBBT or classical beam theory as a result of the works of the Bernoulli's (Jacob and Daniel) and Euler. This model, established in 1744, includes the strain energy due to the bending and the kinetic energy due to the lateral displacement of the beam. In 1877, Lord Rayleigh improved it by including the effect of rotary inertia in the equations describing the flexural and longitudinal vibrations of beams by showing the importance of this correction especially at high frequency [23]. In 1921 and 1922, Timoshenko proposed another improvement by adding the effect of shear deformation [24] [25]. He showed, through the example of a simply-supported beam, that the correction due to shear is four times more important than that due to rotary inertia and that the Euler-Bernoulli and Rayleigh beam equations are special cases of his new result. The former and the thick beam models are the most widely used. The latter accounts for both the effect of rotary inertia and shear deformation, which are neglected when applied to EBBT. The transverse vibration of the beam depends on its geometrical and material properties as well as the external applied boundary conditions. The geometrical properties refer mainly to its length L, size and shape of its cross-section such as its area A, moment of inertia J with respect to the central axis of bending, and Timoshenko's shear coefficient k_y which is a modifying factor to account for the distribution of shearing stress such that effective shear area is equal to $k_y A$. The material properties refer to its density in mass per unit volume ρ, Young's modulus or modulus of elasticity E and shear modulus or modulus of rigidity G. The kinematics of deformation of an element of deflected link with width dx at the position x are show in Fig. 2-1. Due to effect of shear, the original rectangular element changes its shape to somewhat like a parallelogram with its sides slightly curved.

The transversal force and moment equilibrium for the section of an axial loaded beam are given by

$$\frac{\partial V(x,t)}{\partial x} + N\frac{\partial^2 v(z,t)}{\partial x^2} = \rho A\frac{\partial^2 v(z,t)}{\partial t^2} \tag{6}$$

$$S(x,t) + \frac{\partial M(x,t)}{\partial x} = \rho J\frac{\partial^2 \gamma(x,t)}{\partial t^2} \tag{7}$$

Adopting Timoshenko beam theory, the shear force $S(x,t)$ and the bending moment $M(x,t)$ con be expressed as function of $v(x,t)$ and $\gamma(x,t)$. The former is the transverse displacement of the centreline, and the latter is the rotation of the beam cross-section, as shown in *Fig. 2-1*.

$$S(x,t) = k_y GA\left(\frac{\partial v(x,t)}{\partial x} - \gamma(x,t)\right) \tag{8}$$

$$M(x,t) = EJ\frac{\partial \gamma(x,t)}{\partial x} \tag{9}$$

By eliminating $\gamma(x,t)$ from equations (6)-(9), a partial differential equation is achieved, containing the transverse displacement $v(x,t)$ as a single dependent variable:

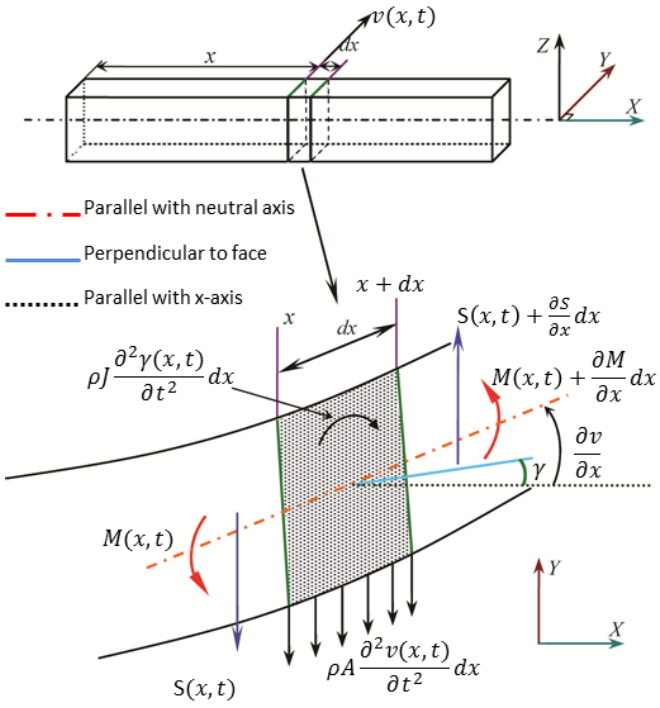

Fig. 2-1: kinematics of deformation of a bending element

$$EJ\frac{\partial^4 v}{\partial x^4} + \frac{EJN}{k_y GA}\frac{\partial^4 v}{\partial x^4} - N\frac{\partial^2 v}{\partial x^2} - \frac{EJ\rho}{k_y G}\frac{\partial^4 v}{\partial x^2 \partial t^2} - \rho J\frac{\partial^4 v}{\partial x^2 \partial t^2} + \tag{10}$$

$$-\frac{N\rho J}{k_y GA}\frac{\partial^4 v}{\partial x^2 \partial t^2} + \rho A\frac{\partial^2 v}{\partial t^2} + \frac{\rho^2 J}{k_y G}\frac{\partial^4 v}{\partial t^4} = 0$$

Eq. (10) is the equation of motion under free vibration and can be transformed into an ordinary differential equation by performing a separation of variables, assuming the transverse displacement $v(x,t)$ to be harmonic at circular frequency ω:

$$v(x,t) = \hat{v}(x)\sin(\omega t) \tag{11}$$

The following ordinary differential equation is achieved by introducing eq. (11) in (10):

$$a\frac{d^4\hat{v}(x)}{dx^4} + b\frac{d^2\hat{v}(x)}{dx^2} + c\hat{v}(x) = 0 \tag{12}$$

Where the parameters a,b e c are defined as:

$$\begin{aligned} a &= EJ\left(1 + \frac{N}{k_y GA}\right) \\ b &= -N + \frac{EJ\rho\omega^2}{k_y G} + \rho J\omega^2 + \frac{N\rho J\omega^2}{k_y GA} \\ c &= -\rho A\omega^2 + \frac{\rho^2 J\omega^4}{k_y G} \end{aligned} \tag{13}$$

The solution of eq. (12) for a fixed value of N is given by:

$$\hat{v}(x) = \sum_{k=1}^{4} C_k \exp(\beta_k x) \tag{14}$$

where

$$\begin{aligned} \beta_1 &= \sqrt{\frac{-b + \sqrt{b^2 - 4ac}}{2a}}, \quad \beta_2 = -\sqrt{\frac{-b + \sqrt{b^2 - 4ac}}{2a}} \\ \beta_3 &= \sqrt{\frac{-b - \sqrt{b^2 - 4ac}}{2a}}, \quad \beta_2 = -\sqrt{\frac{-b - \sqrt{b^2 - 4ac}}{2a}} \end{aligned} \tag{15}$$

The parameters β_i $(i = 1, \dots, 4)$ depend on the bar characteristics: the Young's modulus E, the density ρ, the shear deformation coefficient k_y, the modulus of rigidity G, the cross section A and the geometric moment of inertia J as well. While, the coefficients C_i depend on the boundary conditions, i.e. the constraints.

If both the rotary inertia and shear deformation are neglected, then the governing equation of motion reduces to tat based on the classical Euler-Bernoulli theory, given by:

$$EJ\frac{\partial^4 v(x,t)}{\partial x^4} - N\frac{\partial^2 v(x,t)}{\partial x^2} + \rho A\frac{\partial^2 v(x,t)}{\partial t^2} = 0 \tag{16}$$

In literature, works relied on the more effective results provided by Timoshenko beam theory [8] [12] assume to know k_y as well as G. Generally, the state of the art has been paid about uncertainties on the geometrical characteristics of the tie-rod, on E and ρ, on the constraints behaviour and the effective vibration length of the beam as well, neglecting uncertainties on k_y and G.

2.3 Design of possible methods to estimate axial force in tie-rods

Results achieved by means of TBT analytical solution, as well as based on EBT, rely on the hypothesis of constant cross-section along the beam under investigation. It means to meet restrictions in employing a method which follows that approach, e.g. in any case where screwed coupling joint is present. The approach presented by Garziera et al. [8] suggests away in order to overcome that limit.

The work here described aims to provide a new method capable of providing reliable results, which takes into account the uncertainties on the aforementioned parameters and employable on various types of tie-rods, i.e. not only in a constant cross-section beam case. The new method must provide results as good as the benchmarks in the state of the art, if possible also better than that. The study started by investigating the modal behaviour of a tie-rod modelled as shown in *Fig. 2-2*:

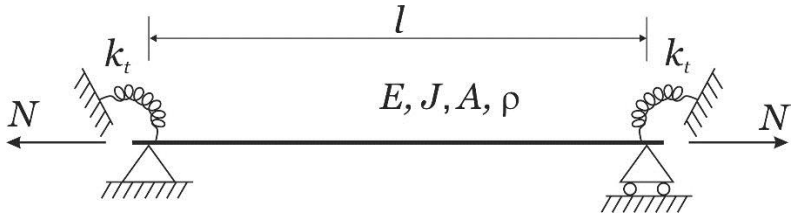

Fig. 2-2: Scheme of the tie-rod

Therefore, if the following hypotheses are considered:

- the structure is symmetric;
- constraints are schematized as two rotational springs (e.g. [9], [6]) with a spring constant named k_t;

- the beam is homogeneous;

then the physical variables influencing beam mode shapes are N, k_t, E, A, l and ρ. The same takes place for eigenfrequencies. As for actual tie-rods, N is of course unknown and the aim of this work is just to estimate it. Usually, the value of k_t is unknown as well. Concerning A, this variable can be measured and thus it is assumed to be known in this work. As for E, ρ and l, they are assumed to be roughly known, meaning that nominal values can be estimated, but their accuracy is poor. In fact:

- the material of the beam can of course be deduced but detailed values of E and ρ can be hardly estimated (especially for ancient tie-rods), unless the material is tested. Therefore, only nominal data can be assigned to E and ρ;

- l can be sometimes difficult to estimate since the ends of the tie-rod could be hidden by other structural elements. Furthermore, when the constraint is soft, the actual beam length taking part in the mode shapes can result longer than its visible portion, as shown in Fig. 2-3 . Therefore, l can be estimated by measuring the visible part of the tie-rod but such a datum could be not accurate.

By taking into account that the actual free span of the tie-rod may be longer than the length measured wall-to-wall allows to overcame the rather restrictive assumption of infinite transversal stiffness at $x(0)$ and $x(l)$, which is rejected by several works (e.g. [4], [10], [12]). As shown in Fig. 2-3, a model providing for an actual length longer than the measured one do not neglect a transversal displacement in correspondence with the positions assumed as beam ends (i.e. the ends of $l_{measured}$). In Chapter 3, the effects of biases on parameters such as l will be investigated, by performing numerical simulations of the tie-rod dynamic behaviour also supposing a length longer than the measured one.

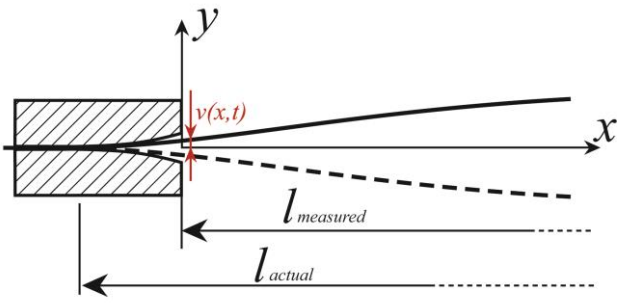

Fig. 2-3: uncertainty on actual vibration length of the beam

Most works in literature require very accurate estimates of E and ρ to assess N (e.g. [11] , [12]). On the contrary, this work assumes that only rough data are available for these two variables, as explained so far.

Before carrying on, it is worth explaining that the stiffness of constraints will be expressed in normalised form from here on, as usually done in literature:

$$k = \frac{k_t}{EJ/l} \tag{17}$$

The next subsection presents the main body of the new method to assess the axial load.

2.3.1 Axial load assessment

The aim of this section is to explain the core of the proposed method. To do this, the effect of N, k_t, l, E and ρ on tie-rod dynamics is investigated. Particularly, their effect on the tie-rod eigenfrequencies is considered. To show such effects, a FE model of a tie-rod was developed. This model employed the more accurate Timoshenko formulation. Such a modelling is not time consuming, so that a lighter formulation with Euler-Bernoulli elements is not necessary [8].

Table 2-1 *r*eports the nominal data used to simulate the tie-rod. Then the five variables were changed singularly step by step and the corresponding values of the first six eigenfrequencies were computed through such a model. The following list shows the ranges used for these variables:

- N ranges between a null load and the yield load N_{YL} (since the yield stress is 300 MPa in this example, then N_{YL} can be computed by multiplying it for the area of the cross-section; see *Table 2-1)*;

- k_t ranges between 0 (i.e simply supported beam) and 300, which is very high and thus very close to a perfect clamped-clamped condition;

- E ranges between -5% and +5% of the nominal value (*Table 2-1*). This is a reasonable variation of the Young's modulus for common steels and common aluminium alloys used in constructions;

- ρ ranges between -2% and +2% of the nominal value (*Table 2-1)*. This is a reasonable variation of the density value for common steels and common aluminium alloys used in constructions;

- l ranges between the nominal length (*Table 2-1)* and l+5% because l is expected to be more likely underestimated than overestimated, as aforementioned;

Fig. 2-4 shows the effect of these five variables on the first six eigenfrequencies. All the five variables influence the eigenfrequency values, especially N and k. The influence of the other variables is low for the first eigenfrequencies (say until the fourth eigenfrequency) and becomes higher and higher as soon as the order of the eigenfrequency increases. This suggests that the first eigenfrequencies could be used to estimate N as soon as an estimation of k_t is available. The influence of E, ρ and l can be neglected as a first approximation. Nevertheless, Chapter 3 will onsider again their effect.

N	K	E	ρ	l	A
$0.5N_{YL}$	150	206000 MPa	7860 kg/m^3	4000 mm	15 x 25 mm^2

Table 2-1: Nominal data for the beam simulated with the FE model. The material is common steel and N_{YL} is the axial load equivalent to the yield stress

Before carrying on, *Fig. 2-5* is provided to stress the concept that both N and k significantly affect the values of eigenfrequecies. This figure shows the numerical solution of the FE model achieved in terms eigenfrequencies (e.g. the first one) according to changes in non-dimensional axial load n and stiffness k. The former parameter is obtained as the ratio between the axial load acting on the model and the nominal yield load (YL) of the material composing it.

The 2D projection of diagram in *Fig. 2-5* is shown in Fig. 2-6, in order to clearly explain the trend of the first eigenfrenquency according to the constraints stiffness and for different values of axial load. Both the variables are able to affect this resonance frequency but the effect of k is greater when its value is lower than about 30. This means that when the constraint condition becomes closer and closer to a simply supported condition, the effect of k increases. On the other hand, when the constraint is that of a nearly clamped-clamped beam (i.e. k higher than 30 [6]), its influence decreases. Similar trends are shown by the other five resonances.

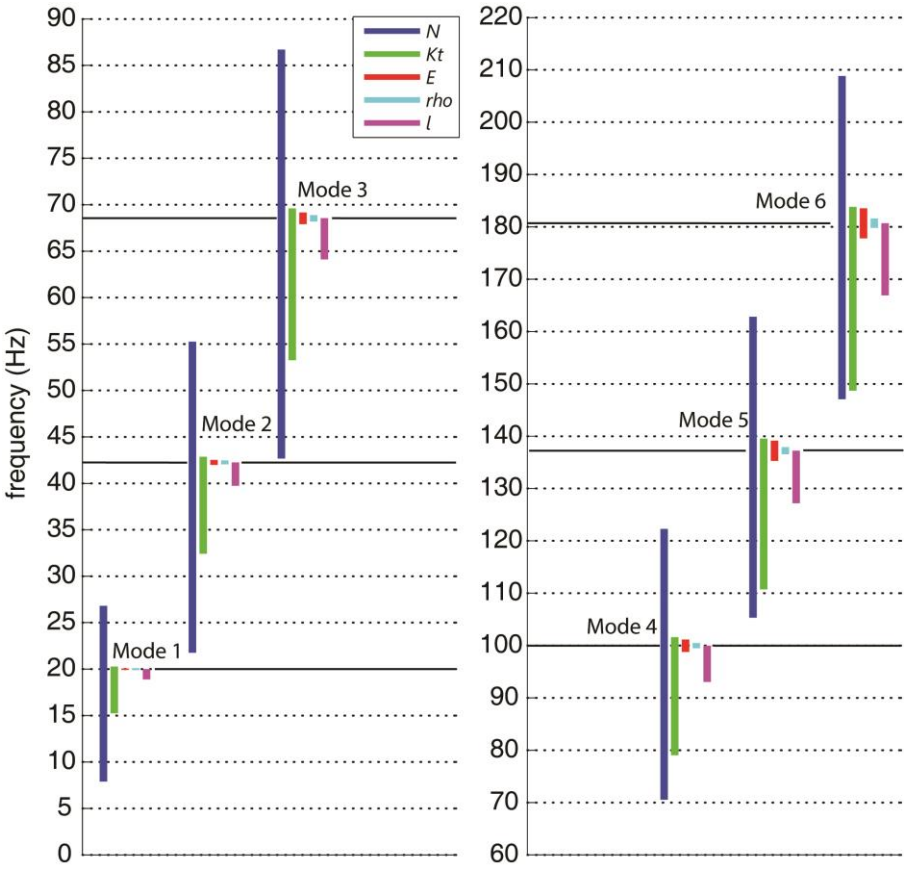

Fig. 2-4: Influence of N, k, l, E and ρ on the first six tie-rod eigenfrequencies

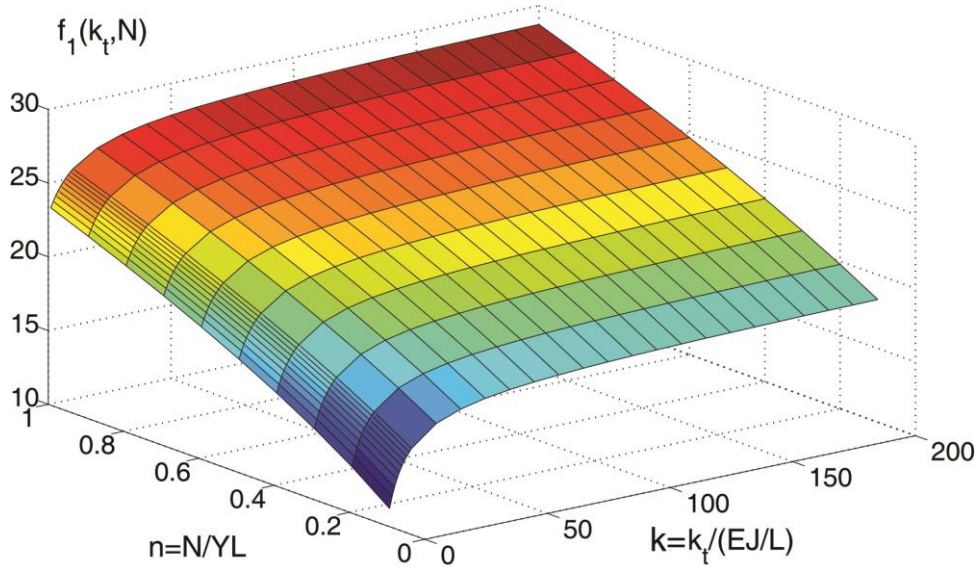

Fig. 2-5: f_1 as a function of non-dimensional axial load and stiffness

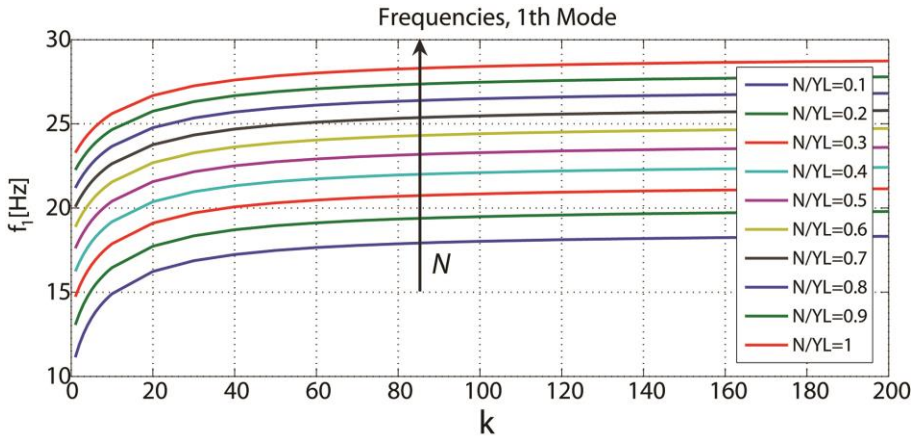

Fig. 2-6: Trend of the first eigenfrequency for the tie-rod descried in Table 1

The results of Fig. 2-6 suggest that the following method could be employed to estimate N:

i. identify the first tie-rod eigenfrequencies by means of experimental tests;

ii. identify k by means of experimental tests and modal analysis (the estimated value will be named k_{est});

iii. build a FE model of the tie-rod where E and ρ are fixed to a nominal value and l is fixed equal to the visible portion of the actual beam. The value of k comes from point *ii* of this list (i.e. k_{est}). A is assumed to be measured. No data about damping must be provided to the FE model and the reason will be clarified in Section 2.4.2.

iv. use the FE model to build the relationship between the value of the eigenfrequencies and N. These curves allow to estimate an axial load N_{exp} for each of the identified eigenfrequencies. Theoretically all the values N_{exp} should be equal but uncertainties, biases and model inaccuracy will prevent such a result and the N_{exp} values will be different each other.

v. find the estimate of N (i.e. N_{est}), which is the value coming from the average of the various values N_{exp} achieved before:

$$N_{est} = \frac{\sum_{i=2}^{n_f} N_{exp,i}}{n_f} \tag{18}$$

Where n_f is the order of the highest considered eigenfrequency, while $N_{exp,i}$ is the estimate of N achieved using the i^{th} eigenfrequency identified experimentally (see point *iv* of this list).

Here n_f is fixed to 4. In fact the first eigenfrequency values are lowly affected by eventual biases on the values of E, ρ and l (*Fig. 2-4*). Although the abovementioned method does not take into account biases on these three variables and uses nominal data, it is very likely that the actual values are different. Thus, the eigenfrequencies over the fourth are not considered in equation (18) to minimise issues related to biases on E, ρ and l (the effect of such biases will be reconsidered in Chapter 3). Actually, another reason for choosing n_f as low as possible exists. The method proposed here is expected to work even with environmental excitation and operational modal analysis and this pulls towards using the first eigenfrequencies since environmental excitation usually shows decreasing power as soon as the frequency value increases. Therefore, it is not recommendable to use high order eigenfrequencies.

Furthermore, the index i in equation (18) starts from 2, instead from 1. The reason is that the value of the first resonance frequency can be highly influenced by the static deflection of the beam. Such a deflection can be considerable when low axial loads are provided to the tie-rod or when the beam is very slender. It is thus recommended in literature [20] to discard the first eigenfrequency when identifying N.

The problem to solve in order to apply the procedure abovementioned is that a reliable technique to estimate k is required (see point *ii* of the previous list). This is faced within the next section.

2.4 Estimation of k

While the assessment of N relies on the resonance frequencies identified experimentally, the estimation of k has been approached by investigating the effects of the constraints stiffness on the mode shapes.

Fig. 2-7 shows the fourth mode shape (chosen as an example) for the same tie-rod used in the previous section (Table 2-1) with different values of k and N. The influence of k is clearly higher than that of N and this suggests to use the mode shapes to estimate k without knowing N. This would allow to carry out the point *ii* of the numbered list of Section 2.3.1.

The information linked to these modal parameters is difficult to manage since each mode shape is a vector of numbers and thus a lot of data should be managed. So, a way to identify the global change of mode shapes due to the constraints behavior by measuring the modal amplitude on a restricted number of points was investigated. In order to do that, two different approaches has been taken into account.

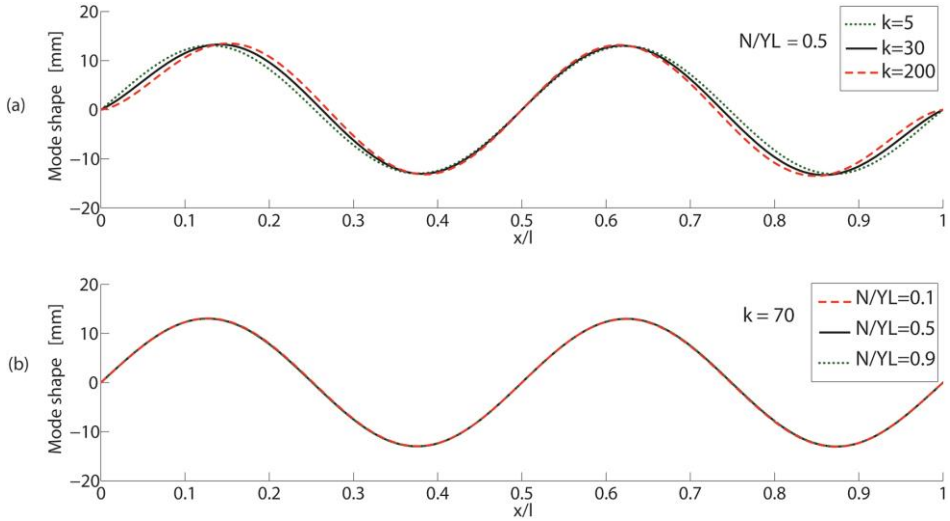

Fig. 2-7: Mode shape with generically scaled values of eigenvector components: for a fixed value of N and different value of k (a), for a fixed value of k and different value of N (b). x is the coordinate along tie-rod length, thus x is between 0 and l.

2.4.1 Identification of k by means of CoMAC

In order to find a synthetic approach capable to show the effect of N and k on eigenvectors, two possible indexes have been identified: the Modal Assurance Criterion (MAC) and the Coordinate Modal Assurance Criterion (CoMAC) [21]. MAC expression is:

$$MAC(i,j) = \frac{\left|\{\phi_X\}_i^T\{\phi_A\}_j\right|^2}{\left(\{\phi_X\}_i^T\{\phi_X\}_i\right)\left(\{\phi_A\}_j^T\{\phi_A\}_j\right)} \tag{19}$$

Therefore, for the i^{th} mode of the modelled tie-rod (i.e. the experimentally-measured mode shape) and the j^{th} mode of a reference structure (i.e. the theoretically-predicted or analytical one), the MAC is calculated by employing the eigenvectors associated to those modes, which are ϕ_X and ϕ_A. The letter T is the transpose operator. The MAC value is 1 when the modes coincide and 0 when there is no correlation between them. Instead, CoMAC-value for degree of freedom i is calculated as follows:

$$CoMAC(i) = \frac{\left(\sum_{g=0}^{L}\left|\{\phi_X\}_i^{(g)}\{\phi_A\}_i^{(g)}\right|\right)^2}{\sum_{g=1}^{L}(\{\phi_X\}_i^{(g)})^2\sum_{g=1}^{M}(\{\phi_A\}_i^{(g)})^2} \tag{20}$$

Here, g represents an individual correlated mode pair, of which a total of L are available. $\{\phi_A\}_i^g$ is the analytic g-mode shape valuated for the degree of freedom i and $\{\phi_X\}_i^g$ is the experimentally-measured one. CoMAC is 1 whether the modes of the two structures are perfectly correlated at the i^{th} point and 0 if no correlation exists.

The mentioned reference structure can be the same tie-rod modelled either in a perfect simply supported condition (Fig. 2-8) or in a perfect clamped-clamped condition (Fig. 2-9). In both cases the axial load is null. Such reference structures can be modelled without making hypotheses about axial load and constraints so that they can be modelled easily.

The MAC trend (with both the mentioned reference structures) for the first six modes has been investigated as a function of k and $n = N/YL$ (where YL is the yield load of the beam) . The same has been carried out for the CoMAC index for all the points of the modelled tie-rod. While the MAC indexes show a behaviour dependent on both k and N, the CoMAC has a trend which is a function mostly of k in some specific points of the structure.

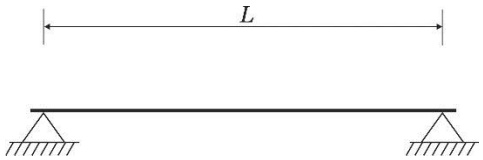

Fig. 2-8: a simply supported (or pinned-pinned) beam

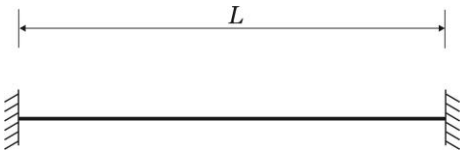

Fig. 2-9: a fully restrained (or clamped-clamped) beam

Assuming a fixed value of k, the CoMAC solutions trend on the normalized rod's span are shown in ***Errore. L'origine riferimento non è stata trovata.*** and Fig. 2-11, respectively, with reference to the pinned-pinned beam model and the clamped-clamped beam model. Trends are evaluated for several values of the axial tensile force N normalized by the yield load YL of the model taken into account. Vice versa, assuming a fixed value of N, the solutions of the same system are shown in *Fig. 2-12* and *Fig. 2-13*, for several value of k. Minimum values of the CoMAC are always close to particular points, which are at about 20% and 80 % of the beam length (i.e. the CoMAC curves for different k values are well separated at about 20% and 80 % of the beam length). These minima do not shift for different loads. Then, *Fig. 2-14* presents the trend of the CoMAC value in these two points as a function of k and n (i.e. the ratio N/N_{YL}) for simply supported-reference structure.

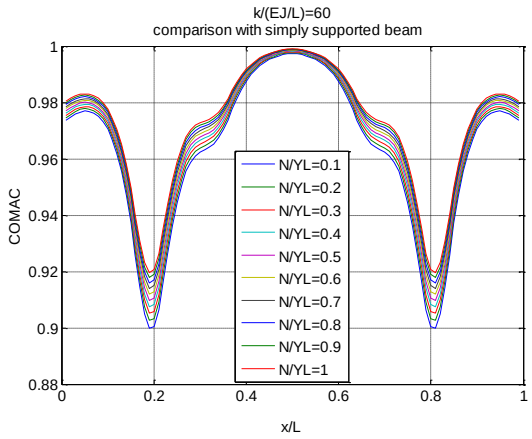

Fig. 2-10: CoMAC index with k fixed, related to pinned-pinned beam

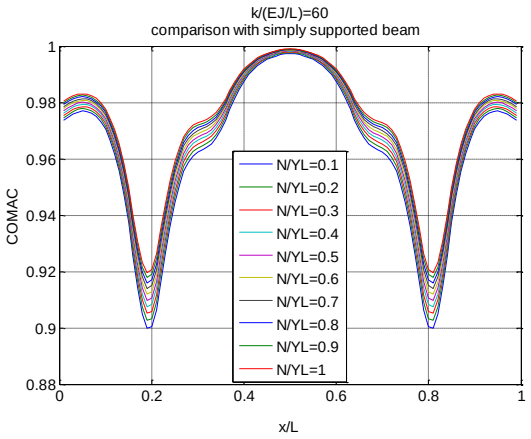

Fig. 2-11: CoMAC index with k fixed, related to clamped-clamped beam

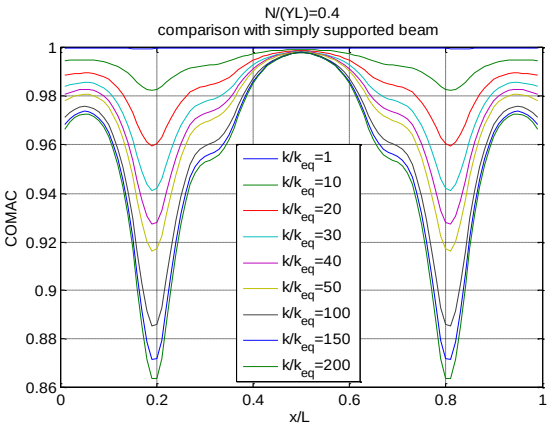

Fig. 2-12: CoMAC index with N fixed, related to pinned-pinned beam

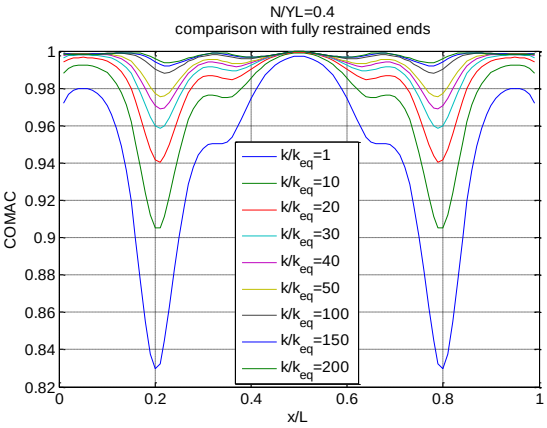

Fig. 2-13: CoMAC index with N fixed, related to clamped-clamped beam

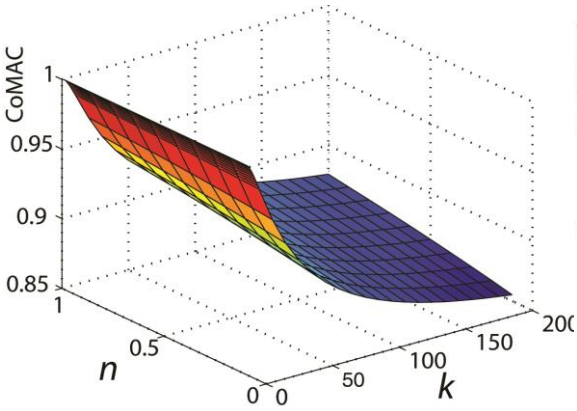

Fig. 2-14: CoMAC minima trend for pinned-pinned beam

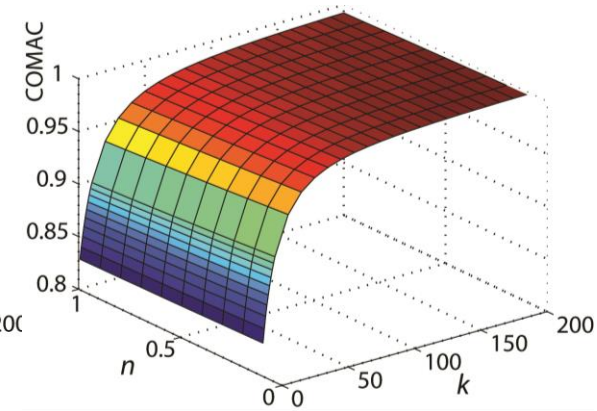

Fig. 2-15: CoMAC minima trend for clamped-clamped beam

It is noticed that the CoMAC value depends almost on the k value only. A similar result concerns the clamped-clamped reference, as shown in *Fig. 2-15.* In the following the points where the CoMAC exhibits the minima will be named x_{min}, while the value of the CoMAC in x_{min}will be named $MINc$.Consequently, the assessment of k can be achieved by means of the following procedure:

i. found the two x_{min} positions by means of the tie-rod FEM (this requires to compute the CoMAC for all the beam points between the structure with generic values of k and n and one of the reference structures; in fact, k and n do not influence x_{min}).

ii. compute of the curve describing MIN_c as a function of k by means of the same tie-rod FEM (a generic n value is used again since it is lowly influencing).

iii. estimate experimentally the eigenfrequencies and the components of the associated mode shapes in x_{min}.

iv. as soon as these experimental data are acquired and the $MIN_c - k$ curve is computed through FEM, the CoMAC value between the actual structure and the modelled reference structure can be calculated and this value is then cross-correlated with the computed curve, allowing to estimate the value of k.

Once k is known, its value can be introduced in the model and the relation between an eigenfrequency (e.g. f1) and n is computed.

From the theoretical point of view, the evaluation of k peformed by cross-correlating the experimental data with both reference structures (i.e. the simply supported beam as well as the clamped-clamped one) should provide the same value of stiffness. Actually, because of uncertainties in the modal identification as well as a non-perfect matching between experimental and numerical models, the method provides two different values of k which are the extremes of an interval including all the possible stiffness of the system's constraints. This range of possible values of stiffness represents the initial guess adopted for performing a modal updating procedure.

This approach relies on the identification of the properly scaled components of the mode shapes. This involves the requirement to measure the input forcing, generally provided by means of an impact hammer. The experimental set-up required for the methods is really simple: it is enough to measure the response in two points, i.e. in the

point of excitation and in one x_{min}. However, the goal of finding a way to assess the k value also employing the environmental forcing led to investigate an alternative suitable approach.

2.4.2 Identification of k by means of the ratio of mode shape components

As Fig. 2-7 shows, the constraints behaviour practically can affect the mode shapes on the whole span of the tie-rod. Fig. 2-16 enlarges a portion in a length portion of the fourth mode shape calculated for the tie-rod described in Table 2-1, evaluated for different values of k. This example is calculated for a generic value of N, but results would be rather equivalent for different value of the axial load, because it poorly affects the mode shaps.

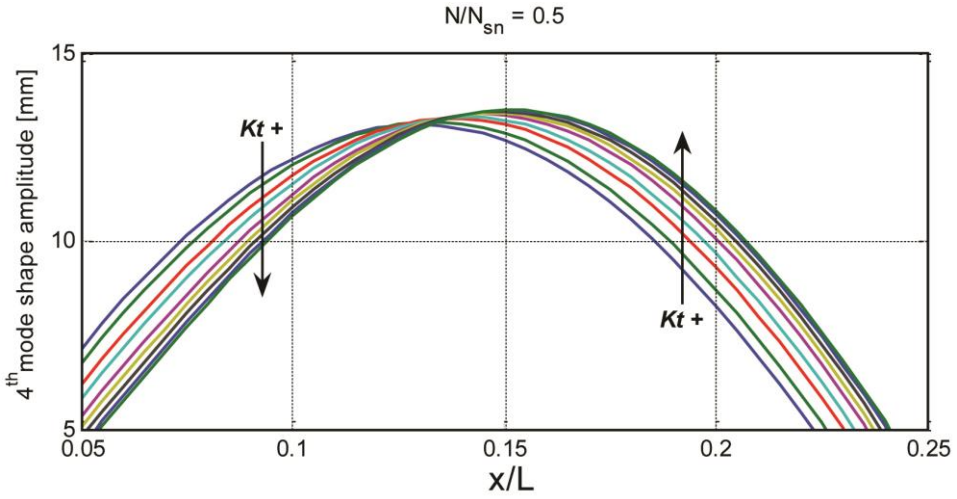

Fig. 2-16: Portions of mode shape with generically scaled values of eigenvector components, for a fixed value of N and different value of k.

The basic idea is to understand whether there are points of the beam where the eigenvector components depend on k and not, or at least lowly, on N. Nevertheless, a deepened approach indicates that the use of the ratio between eigenvector components allows to even employ non-scaled eigenvectors. In fact, if $\phi_{q,y1}$ and $\phi_{q,y2}$ are the scaled eigenvector components of the qth mode at points $y1$ and $y2$ and $\psi_{q,y1}$ and $\psi_{q,y2}$ are the non-scaled eigenvector components of the qth mode at points $y1$ and $y2$, the following relationship is valid:

$$R = \frac{\phi_{q,y1}}{\phi_{q,y2}} = \frac{\psi_{q,y1}}{\psi_{q,y2}} \tag{21}$$

If $\phi_{q,y1}$, $\phi_{q,y2}$, $\psi_{q,y1}$ and $\psi_{q,y2}$ do not depend on N (or are lowly dependent on), also R is not dependent on N. The possibility to use non-scaled eigenvector components allows to even employ operational modal analysis identifications to compute the eigenvectors.

Since equation (18) employs three eigenfrequencies, the corresponding mode shapes are used so that R is defined on three modes, instead on just one to increase statistical reliability (this also increases method sensitivity in estimating k):

$$R = \sum_{q=2}^{4} \left(\frac{\phi_{q,y1}}{\phi_{q,y2}}\right)^2 = \sum_{q=2}^{4} \left(\frac{\psi_{q,y1}}{\psi_{q,y2}}\right)^2 \tag{22}$$

Relying on the previous facts, the y1 and y2 points were looked for by means of the FE model. The R value has been investigated for every couple of positions where the ratio is evaluable (i.e. where the term in the denominator is not close to zero). For example, Fig. 2-17 shows the trend of R calculated with y1 at the 20% of the tie-rod span and y2 at the 10%, for different values of k and N.

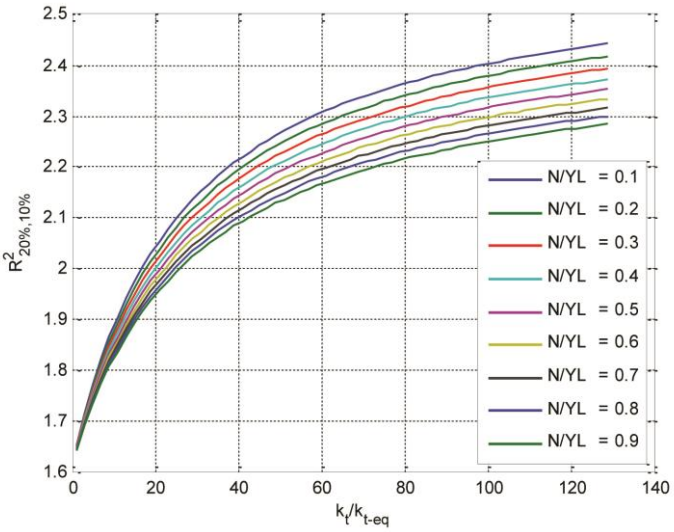

Fig. 2-17: R evaluated al y1=20% and y1=10%, according to different value of k and N

Two criteria were used to choose the best points:

- R must depend on N as less as possible;
- R must depend on k as much as possible so that its sensitivity is maximised.

The coefficients err and m were defined to quantify the dependency of R on N and k respectively. Fig. 2-18 explains how they were computed. Obviously, the $y1$ and $y2$ points were chosen so that err is low and m is high. To facilitate such a task and have a single parameter to consider, a further index was defined (i.e. $ac=err/m$) and this was minimised. All the beam points where at least one of the three modes considered showed an eigenvector component less than 0.1 (where each mode was scaled so that its maximum is 1) were neglected when looking for $y1$ and $y2$ points because their amplitudes are too low and could be affected significantly by measurement noise and identification biases.

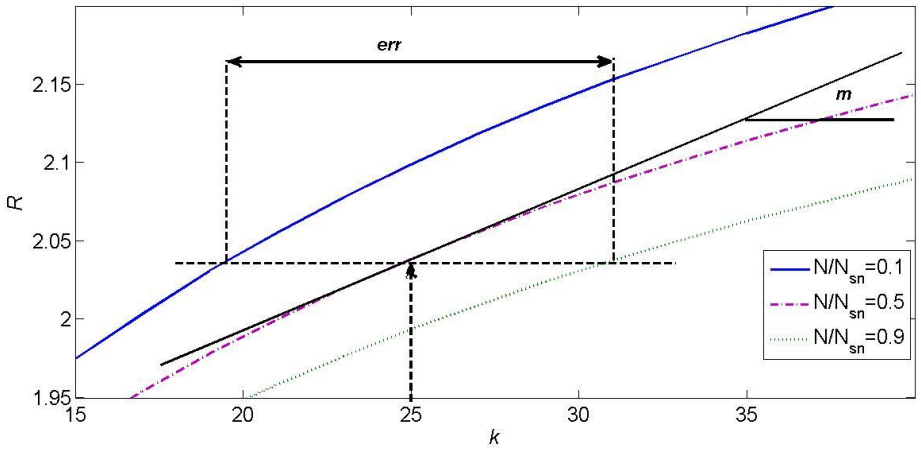

Fig. 2-18: Graphical definition of err and m. The point at 10% and 20% of the beam length were used to build this plot

Finally the following points were chosen:

- y1=9.5% of the beam length;
- y2=3.5% of the beam length;

Therefore, k can be estimated by the following procedure:

a) measure the beam dynamics by means of two accelerometers placed in $y1$ and $y2$ and then estimate $\psi_{q,y1}$ and $\psi_{q,y2}$. Thus, R can be calculated;

b) the FE model is used to build the curve linking k to R. Such a curve is computed fixing E, ρ and l to nominal values, as done in 2.3.1. N is fixed to

$\frac{N_y}{2}$, which is the central value because there are not any clues to choose a different value;

c) finally, the value of k_{est} can be assessed using the abovementioned curve and the value of R estimated experimentally.

The procedures explained in Section 2.3.1 and 2.4 and here to compute N and k respectively do not take into account the uncertainty linked to the estimation of E, ρ and l. Furthermore, N is fixed to $N_{YL}/2$ when estimating k because this is the central value and no other information are available. This constitutes a further bias on the estimated value of k. The next section discusses all these issues.

Previously in this section, the use of the second, the third and the fourth mode shapes were justified by the fact that the corresponding eigenfrequencies were used in section 2.3.1. Nevertheless, there are two important facts which led to the use of these mode shapes. The first is that operational modal analysis is expected to be usable and thus the highest mode shape was fixed to the fourth for the same reasons explained in Section 2.3.1. Then, FE analyses showed that the first mode shape is the most influenced by N and the higher is the mode shape, the lower is the influence of N. This pulled towards neglecting the first eigenmode. The final result is that the modes between the second and the fourth were used.

A final remark regards the fact that damping parameters are not introduced in the FE model. The whole procedure works on eigenfrequencies and eigenvectors. The latters are not affected by the damping value [21], while the formers are lowly affected for usual damping values of metallic tie-rods [21] so that damping is neglected here.

CHAPTER 3

The effect of bias and uncertainty

3.1 Introduction

This chapter is intended to treat the problem of uncertainties associated to the actual free beam length as well as the Young's modulus and density of the material used for making it. Usually, in actual cases the values of E, ρ and l cannot be known accurately and only nominal data are available. In the previous chapter this issue has been temporary neglected in order to investigate a way to estimate k (Section 2.4) and then outline the method described in section 2.3.1.

Observing the results shown by Fig. 2-4, the tie-rod eigenfrequencies look strongly affected by the N as well as k, fairly affected by l and conversely mildly affected by E and ρ. Actually, the simultaneous display of the effects of each parameters makes it hard to appreciate how much E and ρ affect the eigenfrequencies values, because of the wide ranges of variation deemed reasonable for N and $\mathbf{k}$, compared to the $\pm 5\%$ for the Young's modulus and $\pm 2\%$ for the density. Fig. 3-1 draws the attention to the change in frequencies related to E and ρ, related to the tie-rod model defined in Table 2-1 – Section 2.3.1. The uncertainty range accounted for the Young's modulus as well

as the density are reasonable variations for common steels and common aluminium alloys used in constructions. Nevertheless, the more the natural frequencies are high, the more the variations on the mentioned parameters affect the eigenfrequency values. Any shift in frequencies due to bias on the other parameters leads to uncertainties in assessing the axial load by means of the method described in section 2.3.1, but bias on E and l affect the k value by definition (equation (17)) as well. Moreover, the accuracy of both approaches described to assess the value of k (section 2.4 and 2.4.2) are affected by bias on E, ρ and l, due to change in the mode shape. This yields bias on the estimation of k and thus on that of N (Section 2.3).

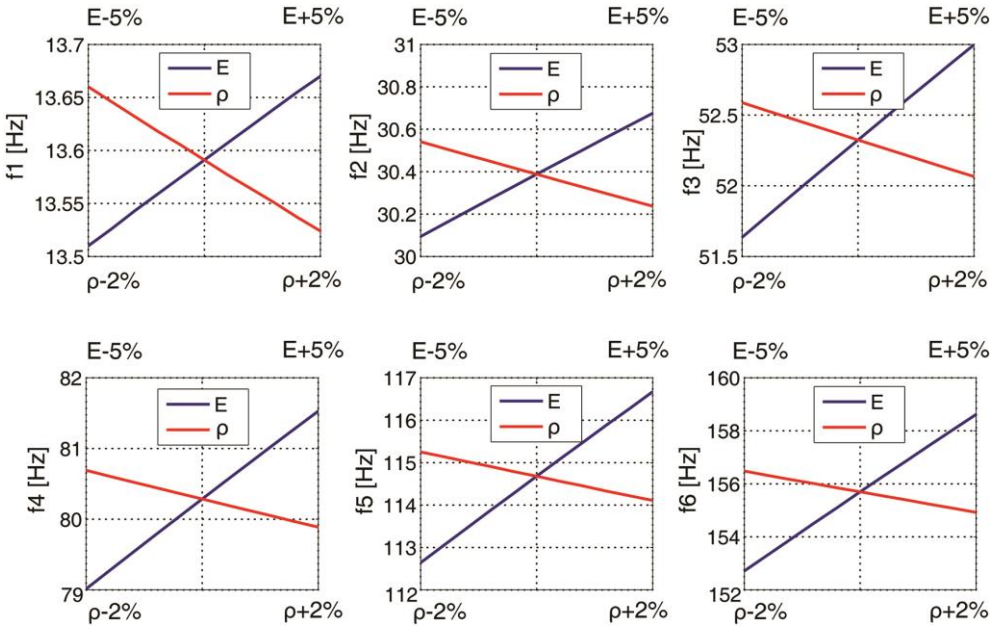

Fig. 3-1: Influence of E and ρ on the first six tie-rod eigenfrequencies (tie-rod model in Table 2-1)

The effect of bias on E, ρ and l was investigate by mean of numerical simulations, which are described in the next section.

3.2 The numerical simulations

Many simulations with FE models were carried out to understand the bias produced on the estimation of k by the uncertainties on E, ρ and l. Different beams - i.e. different lengths, different materials (steel and aluminium alloy), different cross-sections - were simulated to this purpose.

The FE simulations were carried out by developing two models of the beam: one simulated an actual rod (named Model A in the following), while the other was the model on which the approach proposed here relies on (named Model B in the

following). The two models were characterised by different values of E, ρ and l to simulate biases on their estimations. Model B always had nominal values for Young's modulus, density and length, i.e. E_{num}, ρ_{num}, and l_{meas} (Table 3-1). While, model A had different values so that biases were simulated, which is something likely to happen in actual applications (Table 3-1).

Model A				
k	N[N]	E[MPa]	ρ [kg/m³]	l[mm]
–	$0.2N_{sn}$ $0.5N_{sn}$ $0.9N_{sn}$	$E_{nom}-5\% \leq E \leq E_{nom}+5\%$	$\rho_{nom}-2\% \leq \rho \leq \rho_{nom}+2\%$	$l_{meas} \leq l \leq l_{meas}+5\%$
Model B				
$10 \div 100$	$0.5N_{sn}$	E_{nom}	ρ_{nom}	$l_{meas.}$

Table 3-1: Data for Model A and Model B

The values of E and ρ of Model B were chosen so that they represented average values for the considered material (i.e. the nominal values of steel or aluminium) in constructions, while the biases used for Model A were chosen to consider the corresponding extreme values of these variables likely to happen in real construction applications (see the first list in Section 2.3.1). The bias on l is assumed only like a positive increment of the measured length (i.e l_{meas}), since this parameter may be at most underrated in the measurement. These simulations allowed to find out the value of k_{est} (Section 2.4) for different actual values of k (in Model B), by means of the CoMAC index and the ratio R as well.

3.3 Worst case model

In order to provide a reliable analysis of the problem, the worst case scenario in terms of sensibility to the bias on E, ρ and l was looked for. At the moment, both methods described in section 2.4 for evaluating the k value are still taken into account. So the analysis aims to investigate the functions $R_{9.5,3.5}$ (i.e. the ratio of eq. (21) calculated with y_1 equal to 9.5% of the beam length and y_2 equal to 3.5%) and the value of $CoMAC$ assessed against the fully restrained reference model (i.e. the clamped-clamped beam) and the simply supported one as well. These functions will be named R, $CoMAC_{FuRe}$ and $CoMAC_{SiSu}$.

First of all, the effect of the material properties on k estimation are investigated by comparing two FE models which are equal in terms of geometry but made in different

materials, i.e. steel and aluminium alloy. The tie-beam models are 4000 mm long, with a cross-section of 30 x 50 mm. The properties of the material taken into account are shown in Table 3-2, where σ_y is the yield stress and ν is the Poisson's ratio of the material.

	Material	$E\ (MPa)$	$\rho\ (kg/m^3)$	$\sigma_y\ [Mpa]$	ν
Steel model	$Fe430$	200000	7860	300	0.3
Al alloy model	$Al6082$	68670	2690	260	0.3

Table 3-2: Material nominal properties for the models comparison

Both the methods drawn in order to estimate the value of k (i.e. the one based on $CoMAC$ index (Section 2.4.1) as well as the one based on R (Section 2.4.2)) rely on an assumption about the axial load value in the reference model. The $CoMAC$ based method takes into account two unloaded reference models (i.e. the fully-restrained beam as well as the simply-supported one). While, the R based procedure relies on the initial guess that the axial load is equal to $N_y/2$, because this is the central value and no other information are available. Irrespective of the approached employed, the gap between the actual value of N on the real tie-rod and the axial load assumed on the reference model affects the assessment of k. The values of R, $CoMAC_{FuRe}$ and $CoMAC_{SiSu}$ were calculated for both the models in Table 3-2 for different actual value of N, and diagrams in Fig. 3-2 show the results.

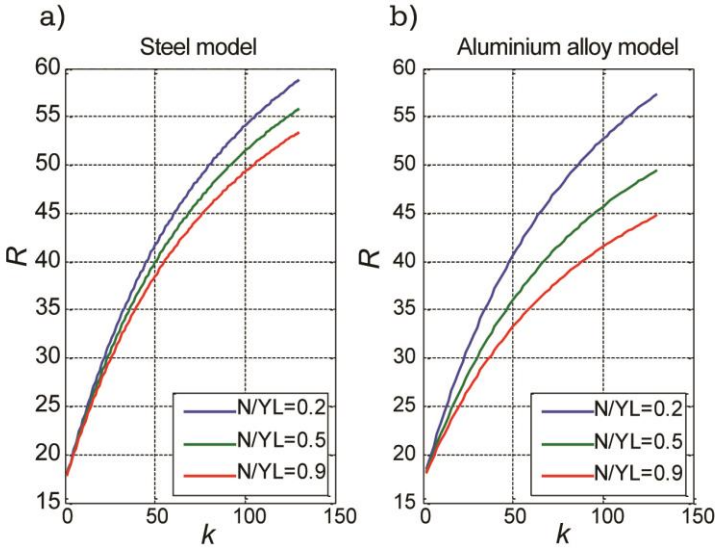

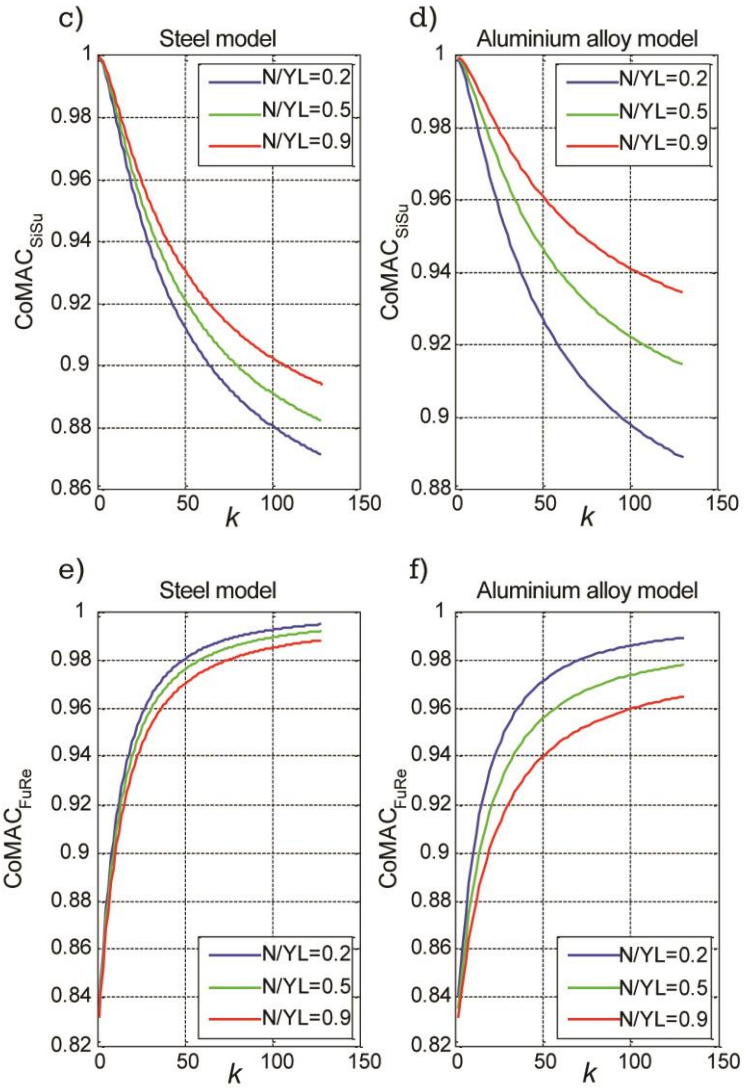

Fig. 3-2: Results in terms of R value for steel made model a) and aluminium made one b); Results in terms of $CoMAC_{SiSu}$ value for steel made model c) and aluminium made one d); Results in terms of $CoMAC_{FuRe}$ value for steel made model e) and aluminium made one f).

The bias achieved for each function according to the change in the N value looks more consistent for the aluminium made model. In order to provide a reliable validation analysis of the method, the worst case scenario has been taken into account. The estimation of k shows more sensitivity to the axial load if the Young's modulus of the material is low, so the aluminium made model represents a critical case.

The geometric properties of the beam model are the other parameters whose effect on the k estimation is investigated. In order to do that, two different aluminium alloy made tie-rod models are compared. The characteristics of the models are shown on

Table 3-3, where j_z is the area moment of inertia and λ is slenderness ratio, which is defined as $\lambda = l/(a \cdot b)$ (a and b are the cross section dimensions and l the length of the beam).

$Tie-Rod$	$Dimensions\ [mm]$	$A\ (mm^2)$	$j_z\ (mm^4)$	$\lambda\ (1/mm)$
$Al.model$ I	30×50	1500	312500	2.67
$Al.model$ II	15×25	375	19531	10.67

Table 3-3: Geometric properties for the models comparison

In order to evaluate how much the slenderness ratio of tie-rod may affect the assessment of k, some FE simulations were carried out to compare the results achieved by means of two models of the beam: one which simulates the biases on the values of N (Model A), while the other is characterized by nominal values of E, ρ and l and a value of N equal to $N_{YL}/2$ (Model B). In this case, biases on E, ρ and l are temporarily neglected, because of the larger range of possible variation assumed for N. So, also Model A assumed nominal values of E, ρ and l. On Model A, the value of k is fixed case by case, in order to define a value of k_{actual}. On Model B, the k value was evaluated, by means of the $CoMAC$ based method as well as the R based one, achieving a value of k_{est} for each method employed. Then, the percentage error on k value was evaluated between the k_{actual} and the corresponding estimated values (i.e. k_{est}):

$$kEr\ [\%] = \frac{100 \cdot (k_{est} - k_{actual})}{k_{actual}} \tag{23}$$

Table 3-4 shows results achieved by numerical simulations for a case characterized by a value of k_{actual} on Model A equal to 35. This value of k matches a critical level of stiffness, because it is an intermediate value between the one close to simply supported case and the one close to fully restrained condition. The results show error values similar for both models of tie-rod. Numerical simulation performed with different values of k on Model A achieved similar results by comparing model I with model II, i.e. the slenderness ratio of the beam basically doesn't affect the assessment of k. These results also show that the k assessment method based on R provides better results than those achieved by means of the $CoMAC$ index based procedure. The advantage of the former method will be discussed in the next section, where the assessment of k will be investigate by taking into account also biases on E, ρ and l.

N real (model B)	*N (model A)*		*kEr % ($CoMAC_{SiSu}$)*	*kEr% ($CoMAC_{FuRe}$)*	*kEr% (R)*
0.2	0.2	model I	0.00	0.00	0.00
		model II	0.00	0.00	0.00
	0.5	model I	14.17	14.24	5.91
		model II	14.19	14.74	5.95
	0.9	model I	38.26	40.55	14.02
		model II	38.26	40.50	14.03
0.5	0.2	model I	-9.06	-8.98	-4.89
		model II	-9.06	-8.96	-4.85
	0.5	model I	0.00	0.00	0.00
		model II	0.00	0.00	0.00
	0.9	model I	14.02	14.76	6.49
		model II	14.02	14.77	6.52
0.9	0.2	model I	-15.30	-15.32	-9.29
		model II	-15.30	-15.32	-9.29
	0.5	model I	-9.10	-9.25	-5.28
		model II	-9.10	-9.24	-5.28
	0.9	model I	0.00	0.00	0.00
		model II	0.00	0.00	0.00

Table 3-4: Error in k assessment for two different geometries of tie-rod (Model A value of $k = 35$)

In terms of geometric properties, the choice fell on a tie-rod model with a lower slenderness ratio. This choice was oriented by the expectation to arrange a test rig with equivalent geometry. A slender tie-rod allows to reach high values of N/N_{YL} (e.g. equal to 0.9) without providing very high absolute values of axial load. A description of this test rig will be dealt in Chapter 5. Due to this analysis, an aluminium alloy made tie-rod characterized by the properties show in Table 3-5 has been chosen for the next numerical simulations.

E	ρ	l	A	σ_y
68670 MPa	2690 kg/m^3	4000 mm	15 x 25 mm^2	260 MPa

Table 3-5: Nominal data of the aluminium alloy beam

Therefore, the results shown hereinafter are those achieved with a very critical tie-rod (Table 3-5), i.e. the aluminium made one.

In order to investigate the assessment of k value, the FE simulations were carried out on two models of the critical tie-rod: one simulated a tie-rod characterized by the nominal value of E, ρ, l and an axial load equal to $N_{YL}/2$ (Model B in Table 3-6), and

the other affected by biases on E, ρ, l and different level of k as well as of N value (Model A in Table 3-6, simulating an actual beam).

Model A				
k	N[N]	E[MPa]	ρ[kg/m³]	l[mm]
–	$0.2N_{YL}$ $0.5N_{YL}$ $0.9N_{YL}$	$68670-5\% \leq E$ $E \leq 68670+5\%$	$2690-2\% \leq \rho$ $\rho \leq 2690+2\%$	$4000 \leq l$ $l \leq 4000+5\%$
Model B				
$10 \div 100$	$0.5N_{YL}$	68670	2690	4000

Table 3-6: Data for Model A and Model B aluminium made tie-rod

3.4 The assessment of k_{est} range

The aforementioned numerical simulations allow to estimate a range of values for k, which is useful for the updating procedure described in the next section. By performing the method described in Section 2.4.1 (i.e. the $CoMAC$ based method) as well as the method described in Section 2.4.2 (i.e. R based method) respectively, two couples of boundary values can be identified (i.e. the critical values of k on the Model A, corresponding to those more affected by biases on the N, E, ρ and l,). These maximum and minimum bounds are named the k_{max} and k_{min} respectively. By evaluating the couples of bounds for each value of k calculated for model B, the functions $k_{max}(k)$ and $k_{min}(k)$ are achieved. These trends can be evaluated by means of $CoMAC$ index method or by that based on R as well. With respect to results in Fig. 3-3, $CoMAC$ index method was applied with reference to the simply-supported beam, but similar results are achieved by means of the clamped-clamped reference as well. Results provided by both methods are compared in Fig. 3-3, which shows the capability of that based on R to provide an interval between the extreme values of k less affected by bias on the other parameters.

First of all, results shown by Fig. 3-3 point out the advantages to employ the method based on R to estimate a range of k values. Many numerical simulations were performed confirming this aspect. Henceforward, that method will be deemed more appropriate for the axial load identification than that based on $CoMAC$ index.

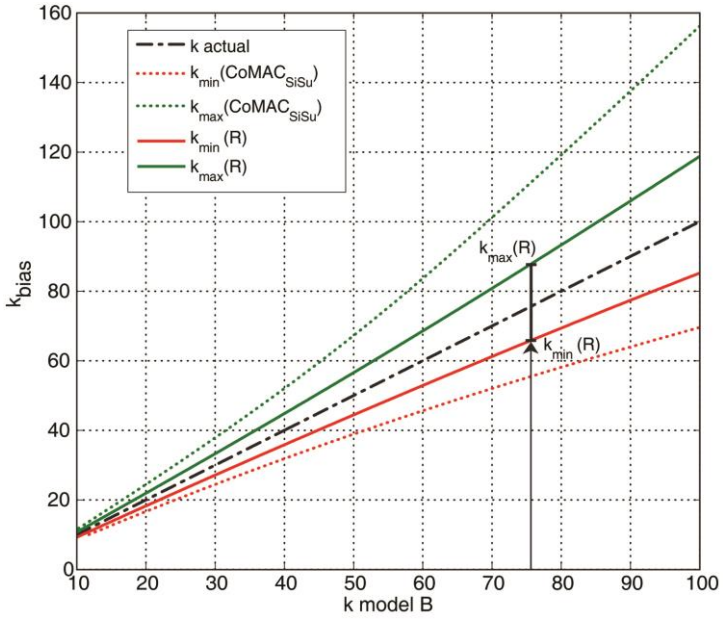

Fig. 3-3: Maxima and minima values of the estimated k values with the bias described in Table 3-6, evaluated with CoMAC and R as well.

Furthermore, the higher the actual value of k is, the higher the maximum bias on k_{est} is. Nevertheless, this is not a big issue. In fact, the estimation of k is required to estimate N. Since the latter variable is estimated by means of the identified eigenfrequencies (Section 2.3.1), it is worth finding out how much the value of k affects the eigenfrequencies. Recalling *Fig. 2-6,* it is evident that the higher k is, the lower the influence on the eigenfrequencies is. Such a behaviour is common to every tie-rod and to every eigenfrequency. Thus, the high biases obtained with high values of k do not represent a big issue.

Now it is worth explaining how the biases shown in Fig. 3-3 can be used to the purpose of identifying N, by referring to the method based on R. Let us suppose to have a real application where to identify the axial load. Two FE models of the tie-rod must be designed, again Model A and Model B. The values of E, ρ and l in Model B are assumed equal to the nominal values associated to the real tie-rod, and N is fixed equal to $N_{YL}/2$. The parameters of Model A are fixed with the same logics used in Table 3-6 (the used ranges can be eventually made narrower if extra-information are available). By accounting for biases on N, E, ρ and l, FE simulations allow to build a figure like Fig. 3-3. Then, k_{est} is computed by means of experimental tests on the real beam. Finally, this estimated value is inserted in the mentioned figure and a range of variation for k is achieved (Fig. 3-4). This plot indicates the possible values of k, taking

into account the biases on N, E, ρ and l. The range of possible values of k will be named r_k in the following and its bounds will be r_{k1} and r_{k2} (Fig. 3-4). As for variable N in Model A (Table 3-6), the bounds could be widened (e.g. to 0.01 N_{YL} and 0.99 N_{YL}) if a higher reliability of r_{k1} and r_{k2} is required for some reasons.

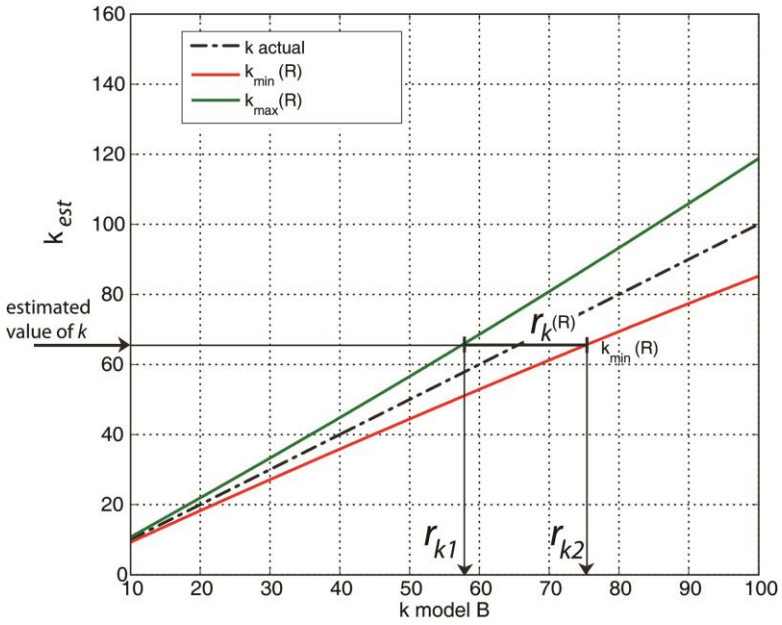

Fig. 3-4: Maxima and minima values of the estimated k values with the bias described in Table 3-6 and the corresponding range r_k with bounds r_{k1} and r_{k2}

The procedures described in Section 2.4.2 and 2.3.1 consider a single value of k to estimate N. The next section explains how the whole method can be improved taking into account the range r_k.

3.5 Enhanced estimation procedure

The previous section explained how a range r_k of possible values for k can be calculated. Furthermore, Section 2.3.1 already discussed how to bound E, ρ and l. This means that four (i.e. k, E, ρ and l) of the five problem variables can be bound. The benefits provided by bounding k through r_{k1} and r_{k2} are evident looking at *Fig. 3-5*: this plot is equal to that in *Fig. 2-4* (for the beam of Table 2-1) and it shows that the addition of bounds on k decreases very much its influence on the eigenfrequency values and thus on the estimation of N.

Some papers referenced in Chapter 1 (e.g. [8], [9]) suggested axial load identification method based on model updating procedures. A similar approach can be used to refine the estimates of k and N coming from the procedures given in Section 2.3.1 and Section 2.4.2.

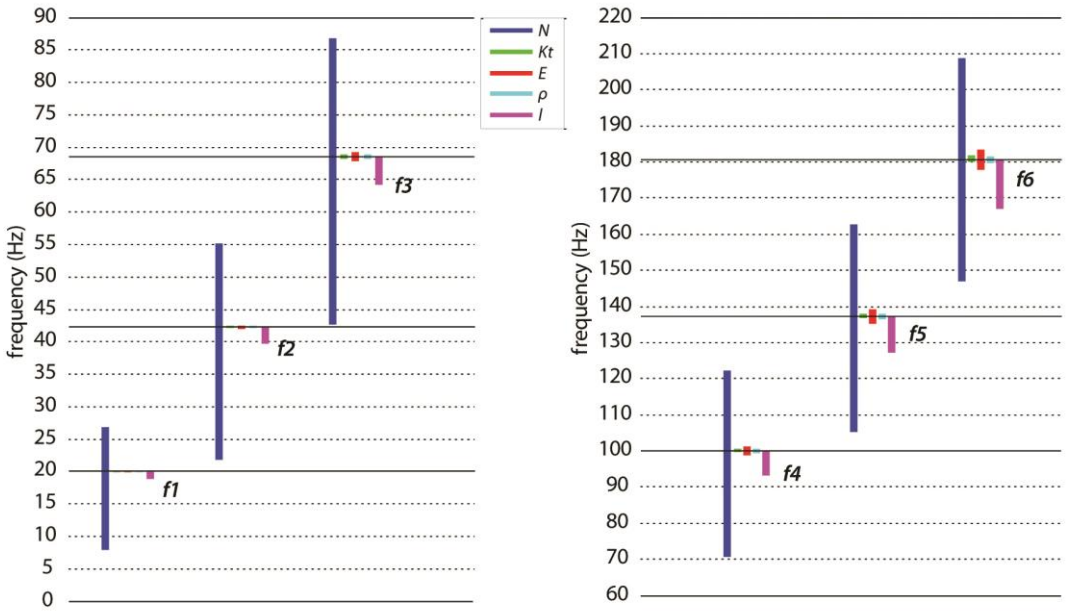

Fig. 3-5: Influence of N, k, E, ρ and l on the first six eigenfrequencies for the tie-rod of Table 2-1 and with bounds r_{k1} and r_{k2}

One of the advantages of the method here proposed is to provide a bounded range of k values. The model updating procedure here employed requires to minimise a function z, which depends on the numerical and experimental eigenfrequencies:

$$z = \sum_{i=2}^{4} \left(f_{num,i} - f_{exp,i}\right)^2 \tag{24}$$

Where $f_{num,i}$ is the ith numerical eigenfrequency calculated through the FE model and $f_{exp,i}$ is the ith eigenfrequency identified experimentally. The function z is minimised by changing the values of N, k, E, ρ and l. As explained above (Section 2.3.1), three eigenfrequencies taken into account (i.e. from the 2nd to the 4th), whereas the updating procedure works on 5 variables. This is explained by paying attention to Fig. 3-5, which shows that the eigenfrequency values basically are affected by N and l, slightly affected by E and ρ (mostly from the 1st frequency to the 4th one), while the effect of k is reduced by bounding it through r_{k1} and r_{k2}. This means that there are just two

variables affecting the value of z and the minimization on three eigenfrequencies is enough accurate. Nevertheless, the number of eigenfrequencies used can be increased, Just three eigenfrequencies will be employed from now on in order to test the updating procedure in the worst scenario.

The first trial values and the bounds are given in Table 3-7 and they comes from the facts explained before. Particularly, the starting values for N and k are achieved by means of the algorithms described in Section 2.3.1 and Section 2.4.2 respectively. Furthermore, the bounds of k are r_{k1} and r_{k2} (Section 3.4). The algorithm used here for the updating is the interior point.

Starting values	k	k_{est}	Bounds	k	$r_{k1} \div r_{k2}$
	$N\ [N]$	$N_{YL}/2$, where N_{YL} comes from the usual nominal value of the yield stress for the considered material (e.g. 300 MPa for steel)		$N\ [N]$	$0 \div N$
	$E\ [Mpa]$	Usual nominal value (e.g. 200000 for steel and 68670 for aluminium alloys)		$E\ [Mpa]$	Starting value $\pm 5\%$
	$\rho\ \left[\frac{Kg}{m^3}\right]$	Usual nominal value (e.g. 7860 for steel and 2690 for aluminium alloys)		$\rho\ \left[\frac{Kg}{m^3}\right]$	Starting value $\pm 2\%$
	$l\ [mm]$	Length of the visible portion of the beam		$l\ [mm]$	Starting value $+ 5\%$

Table 3-7: Starting values and bounds for the updating procedure

This refined method has been tested numerically and then experimentally. The numerical verification is discussed in the next chapter, while the experimental activity is shown in chapter 5.

CHAPTER 4

The Numerical validation of the method

4.1 Introduction

The previous chapter explained how to manage the uncertainties affecting the parameters involved in the method outlined in section 2.3.1. A set of reasonable bounds are defined for E, ρ and l. Then, the biases on these parameters are used to define a method to assess the bounds of k as well, by assuming an axial load value equal to $N_{YL}/2$. The set of values (or ranges) of N, k, E, ρ and l represents the first guess for the optimization algorithm which aims to minimize the function z defined by equation (24). Based upon these analysis, the procedure defined on page 29 can be tested in order to validate its effectiveness.

Firstly, a cost-effective way to perform a wide-scale validation is to rely on numerical simulations which take into account a large number of potential situations. This approach allows to simulate some case stadies of tie-rod, subjected to different value of axial load and taking into account biases on k, E, ρ and l as well. A Montecarlo simulation represents an ideal way in order to study the effects of statistic distributions of some parameters which characterize the model of tie-rod investigated [26]. This approach requires the analysis of a very high number of case studies. Due to the time consumption required by perform each FE simulation as well as to compute the results,

the validation described in the next section was provided by running 200 simulation for each combination of N and k applied to each case study. The updating procedure performed has shown a convergence of the parameters under investigation towards reasonable ranges, ensuring a reliable evaluation of the proposed method.

4.2 Case studies

Two case study tie-rods were chosen to test the method numerically. Their nominal features are provided in Table 4-1.

	E [MPa]	ρ [kg/m^3]	l [mm]	A [mm^2]
Tie-rod 1	*68670*	*2690*	*4000*	*15 x 25*
Tie-rod 2	*200000*	*7860*	*10000*	*30 x 50*

Table 4-1: Nominal data of the tie-rods used for simulations

The first of them (i.e. that in aluminium alloy) was tested on 9 cases, while the other (i.e. that made up of steel) in 4 cases (Table 4-2). Therefore 13 different simulations were performed. Each simulation consisted of 200 runs and these runs followed this procedure:

i. Model A and Model B of the tie-rod were built (refer to Chapter 3 for the description of Model A and Model B). The values of E, ρ and l were fixed according to Table 4-1 for Model B (i.e. these values are average values for common steel and aluminium used in constructions). As for Model A, N and k were fixed according to Table 4-2 and on each run the values of E, ρ and l were fixed by means of extractions from rectangular distributions, whose bounds are defined in Table 4-3;

ii. the procedures explained in Section 2.3.1, Section 2.4.2 and Section 3.4 were carried out to have first trial values of N and k and to estimate r_{k1} and r_{k2};

iii. the model updating procedure (Section 3.5 and Equation (24)) was performed on Model B, reaching a final value of the five variables;

iv. the estimated variables were compared to the values fixed for Model A (i.e. the true values).

	N	k
Tie-rod 1	$0.2\ N_{YL}$, $0.5\ N_{YL}$, $0.8\ N_{YL}$	$25, 35, 70$
Tie-rod 2	$0.2\ N_{YL}$, $0.8\ N_{YL}$	$25, 70$

Table 4-2: Case-studies for the simulations

	E [MPa]	ρ [kg/m^3]	l [mm]
Tie-rod 1	Nominal value (Table 4-1) $\pm 5\%$	Nominal value (Table 4-1) $\pm 2\%$	l (Table 4-1) $\div\ l + 5\%$
Tie-rod 2	Nominal value (Table 4-1) $\pm 5\%$	Nominal value (Table 4-1) $\pm 2\%$	l (Table 4-1) $\div\ l + 5\%$

Table 4-3: Bounds for statistical extractions

As aforementioned, the values of E, ρ and l of Model A are extracted from a rectangular statistic distribution spread in the boundary of Table 4-3. Fig. 4-1 shows an example about the distribution of E assumed for the aluminium tie-rod model.

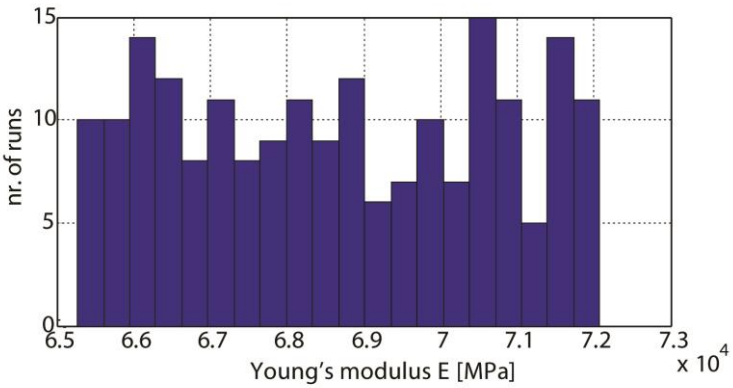

Fig. 4-1: destribution of Young's mosulus for Tie-Rod 1 in Table 4-3

4.3 Numerical validation results

First of all, for each case study, the simulation described in the point ii of the numbered list in Section 4.2 provides 200 results in terms of first trial values of N. Secondly, point iii optimizes the values of N, E, ρ and l for each run. The true values fixed for each case study allow to evaluate the reliability of the updating method. The results of comparison are evaluated in terms of errors Er between the true values of N (i.e. N_{ref}) and the corresponding estimated values (i.e. N_{est}):

$$Er\ [\%] = \frac{100\left(N_{est} - N_{ref}\right)}{N_{ref}} \tag{25}$$

The distributions of results in terms of Er on the axial load were evaluated. Er can be calculated before performing the updating procedure (i.e. N_{est} is the axial load achieved by employing the method in Section 2.3.1) or after the procedure (i.e. N_{est} is the optimized axial load value). For example, for a case study characterized by $N/N_{YL} = 0.8$ and $k = 25$, the Er values are show in Fig. 4-2, before and after the updating procedure respectively. The distribution was also evaluated in terms of average value of Er (e.g. $\overline{Er_{\%}}$) as well as by standard deviation σ_E, which measures the spread of the data. The results achieved after the updating procedure show a distribution close to a normal distribution function. In that condition, the average value represents the proper expected value of the statistic distribution and the spread of the data can be properly defined by twice the standard deviation (i.e. $2\sigma_E$) [27].

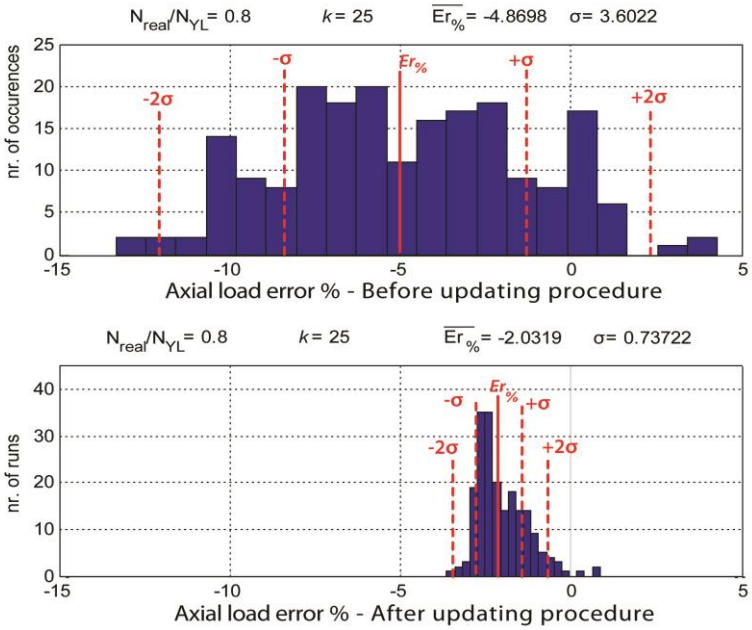

Fig. 4-2: distribution of N/N_{YL} achieved by Montecarlo simularions, before and after updating procedure

Fig. 4-3 shows the resulting distributions about all case studies investigate for aluminium tie-rod model (i.e. 9 cases), after the updating. The results of 200 Montecarlo simulations relative to most of the cases investigated show a very narrow distribution of Er, close to normal one. In terms of accuracy, the statistical analysis of a normal distributed ensemble can be expressed by the average value of Er and the interval defined by plus and minus twice of the standard deviation (i.e. $2\sigma_E$) [27]. It may be assumed that by increasing the number of simulation for each Montecarlo analysis the distribution of results achieved by the updating axial load identification become closer and closer to a normal one.

Irrespective of the possibility to define a statistical distribution of the results, the spread of Er values for each set of simulation can be defined by the range between the minimum and the maximum Er achieved the updating procedure. This approach assures a reliable expression of the result accuracy. Therefore, results in terms of average value of $\overline{Er_{\%}}$, $\pm 2\sigma_E$ interval and the boundary values Er_{max} and Er_{min} are shown in Fig. 4-4 before and after the model updating task. This figure shows that the method tends to underestimate the axial load and this due to the effect of variable l. In fact, l can be underestimated but not overestimated (Table 4-1) by Model B. Nevertheless, the updating allows to decrease very much the bias on the estimation of N. The most critical situation is that characterised by low loads, as usual in most of the referenced works. Anyway, the maximum bias is a bit more than 10% in the worst case. Such a case is that characterised by the maximum bias on l, E and ρ.

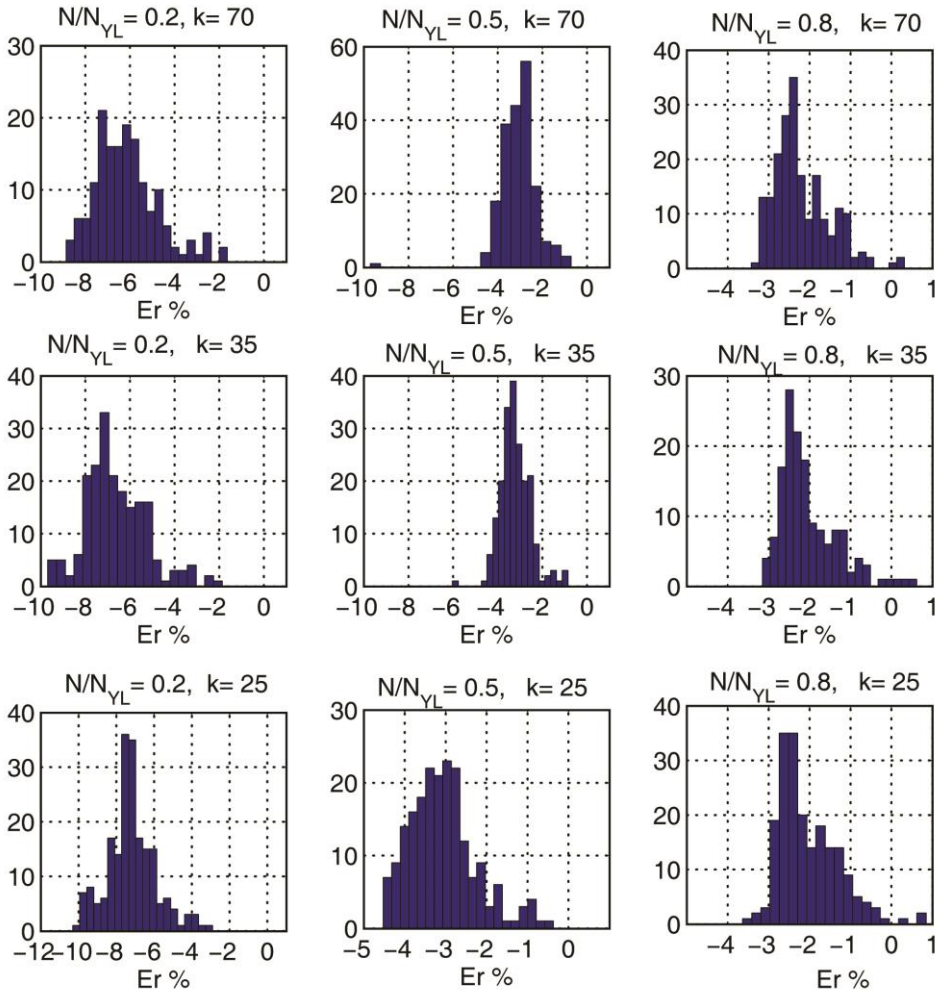

Fig. 4-3: Distributions of the errors in N estimations after the updating procedure (aluminium tie-rod)

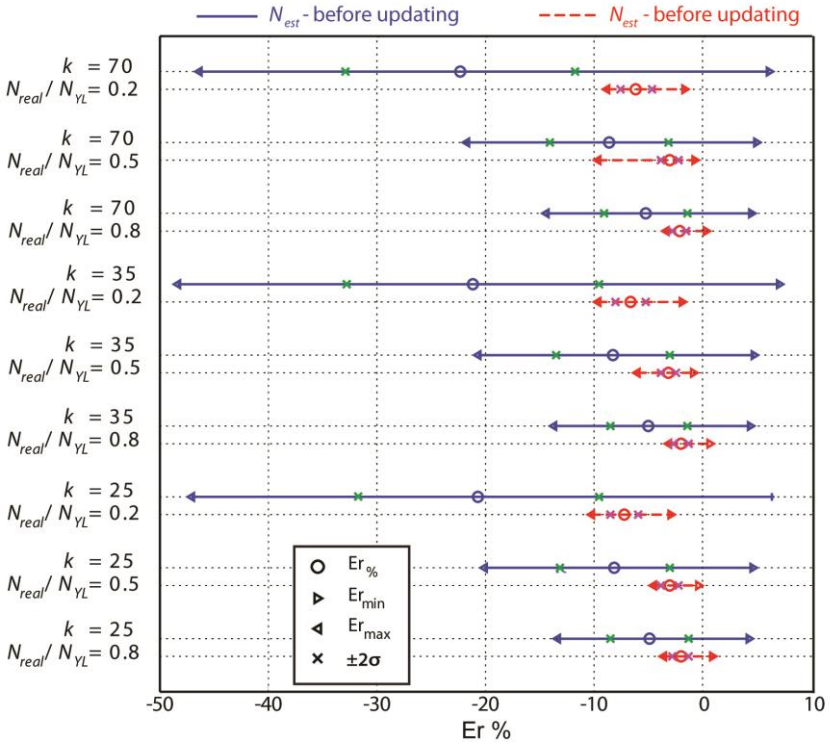

Fig. 4-4: Errors in N estimations before and after the updating procedure (aluminium tie-rod)

An example about what happens for the value of k, l, E and ρ after the updating procedure is shown in Fig. 4-5. It is reminded that a rectangular statistical distributions is assigned them, bounded by values in Table 3-7, before updating.

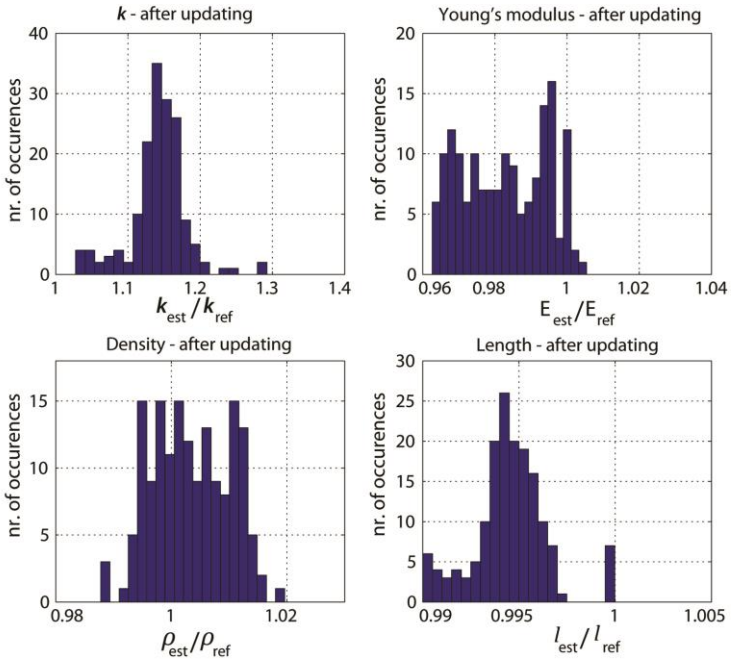

Fig. 4-5: E, ρ and l distribution after updating procedure ($N = 0.2N_{YL}$, $k = 70$)

It is not worth to define a proper statistical distribution about this parameters, but it is essential that the values obtained are in a reasonable range. Even if k and l offer a distribution of errors very close to a normal one, for these parameters as well as for E and ρ the accuracy of results in term of error are provided by the value of $\overline{Er_{\%}}$ and the boundary values Er_{max} and Er_{min}.

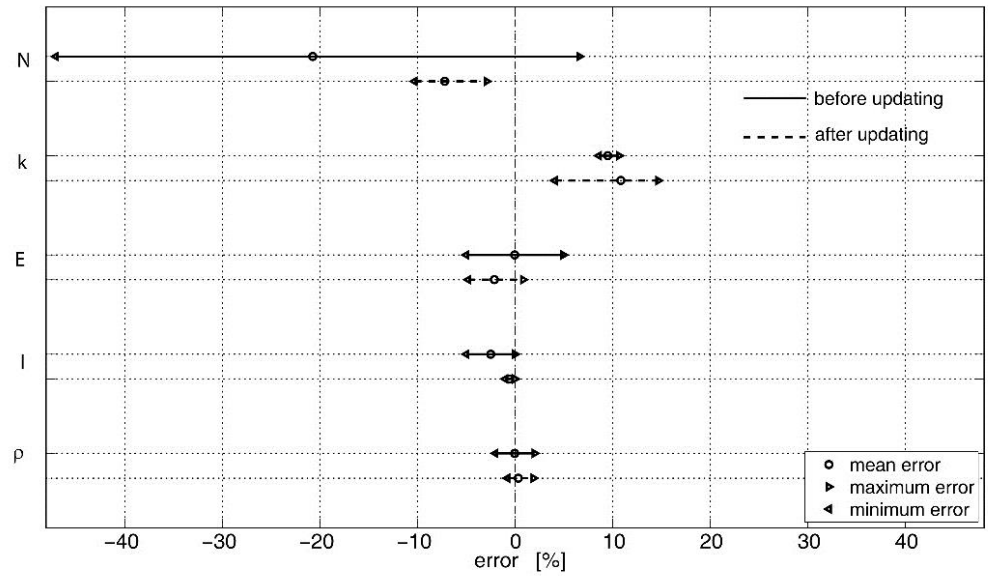

Fig. 4-6: Results for all the variables for the simulation with k=25 and N=0.2N_{YL} (aluminium tie-rod)

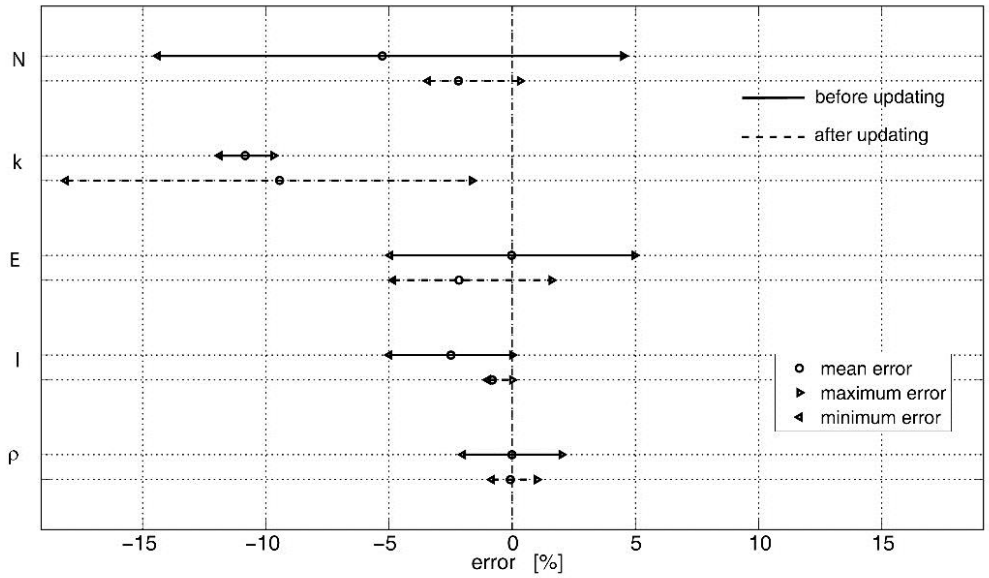

Fig. 4-7: Results for all the variables for the simulation with k=70 and N=0.8N_{YL} (aluminium tie-rod)

Fig. 4-6 and Fig. 4-7 show the estimated values for the other problem variables (i.e. k, l, E and ρ) for two simulations, chosen as examples. The mean estimated value of the other variables often tends to the true value and thus the method proposed demonstrates to be reliable. A slight tendency to underestimate E is evident and it is mainly due to the underestimation of l.

4.4 Conclusion

A method for indirect axial load assessment in a tie-rod was outlined in Section 2.3.1. It initially relies on a set of starting values of N, k, l, E and ρ evaluated for the tie-rod under investigation. Secondly, dynamic measurements assess three eigenfrequencies (from the 2nd to the 4th) and the relative mode shape components are identified in two chosen positions. Thirdly, A FE model of the tie-rod is designed in order to perform numerical simulations by assuming two different sets of parameters (Model A and B). Then, mode shape component are employed to assess a range of values for k by means of the numerical simulations, also taking into account biases on N, l, E and ρ. Therefore, a first value of N is calculated by mean of the eigenfrequencies. Finally a model updating procedure in performed in order to refine the estimates of N. This procedure has been numerically tested by means of Montecarlo simulations, performed on different case studies. These cases are related to an aluminium made tie-rod model and a steel made one as well.

Table 4-4 presents a summary of the numerical validation results. Montecarlo simulations are performed on the steel made tie-rod model as well. Also in this case, the method shows to be effective and reliable (Table 4-5).

N/N_{YL}	k	$\bar{E}_r$ [%]	σ [%]	E_r^{min} [%]	E_r^{max} [%]
0.2	25	-7.21	1.30	-10.30	-2.90
	35	-6.63	1.39	-9.68	-2.87
	70	-6.14	1.41	-8.86	-1.64
0.5	25	-3.07	0.84	-9.70	-0.72
	35	-3.20	0.69	-6.02	-0.85
	70	-3.07	0.81	-4.52	-0.37
0.8	25	-2.18	0.69	-3.42	0.32
	35	-2.04	0.71	-3.15	0.62
	70	-2.03	0.74	-3.64	0.85

Table 4-4: Results for the estimates of N after the updating procedure (aluminium tie-rod)

N/N_{YL}	k	$\bar{E}_r$ [%]	σ [%]	E_r^{min} [%]	E_r^{max} [%]
0.2	25	-7.73	1.05	-10.58	-2.85
	70	-7.65	0.78	-9.65	-3.22
0.8	25	-1.79	0.73	-3.65	0.37
	70	-1.72	0.78	-3.33	0.43

Table 4-5: Results for the estimates of N after the updating procedure (steel tie-rod)

The method present here takes into account biases on the parameters of the tie-rod which affect its dynamic behaviour (i.e. k, l, E and ρ) larger than those treated by most of the referenced works. In spite of this, the results provided by the numerical validation show to be as reliable as the best performing methods. Furthermore, the results of the numerical simulations are more reliable than those reported for the best referenced methods in given cases.

The next Chapter validates the method experimentally.

CHAPTER 5

The Experimental validation of the method

5.1 Introduction

This section faces the experimental validation of the proposed technique. A tie-rod made of aluminium was realised in laboratory with the measured values described in the first raw of Table 5-1. The features of such a beam were chosen to test the method under critical condition (i.e. aluminium was chosen to have a low Young's modulus and the tie-rod geometry to have a slender case-study beam; see section 3.3). The FE model of the beam was realised by fixing the nominal data in the second raw of Table 5-1. Therefore, biases are introduced intentionally on l and E. The actual value of ρ was not measured because its influence is really low (e.g. Fig. 3-5). The Young's modulus was experimentally assessed in situ by means of a load cell (which provides the axial load) and a strain gauge bridge fixed on the beam (which provides the strain).

	$E\ [MPa]$	$\rho\ [kg/m^3]$	$l\ [mm]$	$A\ [mm^2]$
Real Tie-rod	*66552*	*2690*	*3996*	*15 x 25*
FE model	*68670*	*2690*	*4000*	*15 x 25*

Table 5-1: characteristics of the tie-rod for experimental validation (real beam a FE model)

A difference between simulations (Chapter 4) and experimental tests is that in the latter case an overestimation of l (i.e. nominal value higher than the actual value) is considered, while in the former case only underestimations were considered. Such a

choice comes from the will to fully test the method when a bias on the measurement of the visible portion of the beam takes place.

5.2 Test rig

In order to design a flexible test rig, which allows to simulate different condition of axial load as well as different behaviour of the constraints, some requirements were taken into account:

i. the axial load must be easily variable and continuously measured with accuracy;
ii. the constraint layout must ensure a change in the torsional stiffness and design aiming to simulate a wide range of variation. Ideally the bounds should extend from a conditions close to a clamped-clamped case to opposite, close to a simply supported case;
iii. the layout must ensure also high level of axial load, at least equal to $0.7N_{YL}$.

In order to enable any longitudinal translation of the beam, a way to fix the ends ot the beam must be find. In case of circular cross-section beam this requirement is ensured by means of a screw-bolt at the ends. This solution is impossible in case of rectangular cross-section. Few dowels are required in the portion of the beam clamped by the constraints, in order to enable any longitudinal translation (i.e. ensure that the beam can bear an axial load). In correspondence with the holes in the beam for lodging the dowels, the cross-section is resized, therefore the critical condition of attaining a yield stress in that section is real, if the axial load applied in close to N_{YL}. In order to avoid any problem, the beam was design with a larger cross-section area in correspondence of the clamp, as show in Fig. 5-1.

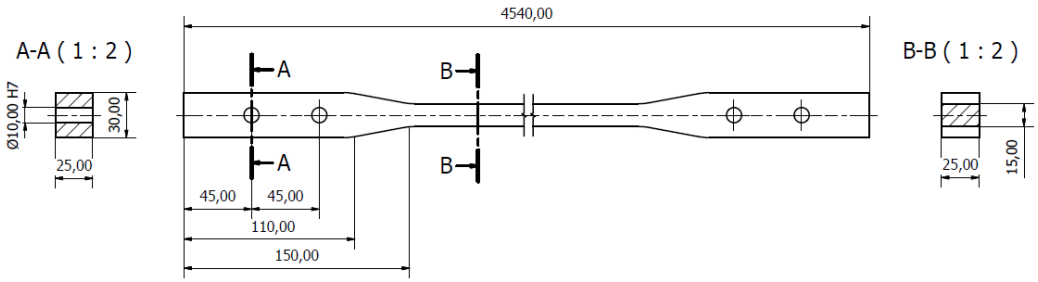

Fig. 5-1: change in cross-section area in the beam ends for the dowels lodging

The clamps were designed in a modular layout, to allow a change in the torsional constrain provided to the tie-rod. This task was carried out also by interposing some rubber layers between the clamp element and the beam, in order simulate also a lower level of stiffness provided by the constraints. One of the clamps is able to have a longitudinal shift when its bolds are not tightened, in order to ensure a change in the strain applied on the beam (Fig. 5-3). In fact, this clamp is connected also to another beam which is tense by means of a screwed coupling joint. On this side, a load cell is placed serially to the screwed coupling joint. This device ensures a very accurate measurement of the axial load. Fig. 5-2 shows the whole set up for experimental tests.

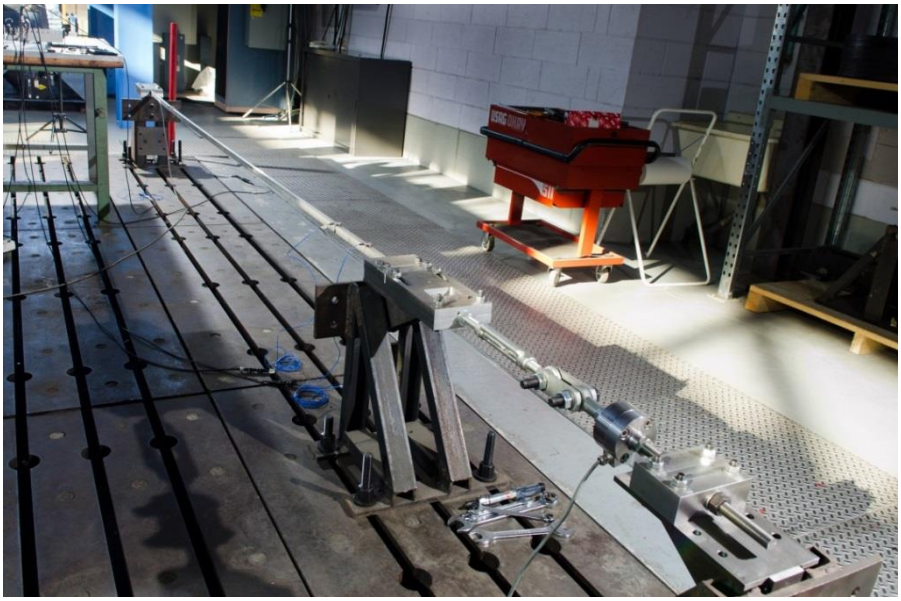

Fig. 5-2: tie-rod layout for experimental validation. In the foreground (in the lower right) the load cell and the screwed coupling joint are visible.

When the bolts on the clamp are tightened, the measurement provide by the load cell loses reliability. To overcame this problem, a strain gauge bridge was placed in the tie-rod span (Fig. 5-4). The Strain gauge configuration was a full-bridge sensitive to axial strain.

The full-bridge layout ensure higher sensitivity to the strain and at the same time compensates for any temperature drift. The strain gauge bridge was calibrated by means of the load cell and the measurements of both devices are compared every time the axial load has been change, before tightening the clamp placed between the tie-rod and the beam connected to the load cell (i.e. when the two sections are subject at the same axial load).

Vibration measurements are made by three piezoelectric accelerometers PCB 333B30 (see Fig. 5-5), which metrological specifications are shown in Table 5-2. The specifications of such a device ensure a good trade-off between few requirements: low weight to avoid any loading effect on the beam; full-scale enough for measuring the hammer impact response but sensitivity high enough as well as a signal/noise ratio as good as possible to provide accurate measurements also during tests with environmental forcing.

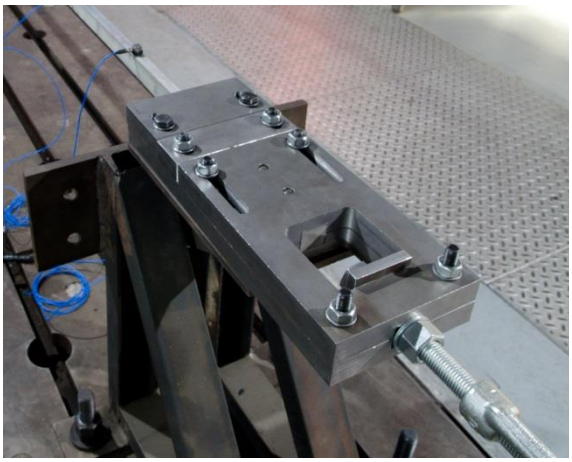

Fig. 5-3: the clamp connected to the screwed coupling joint

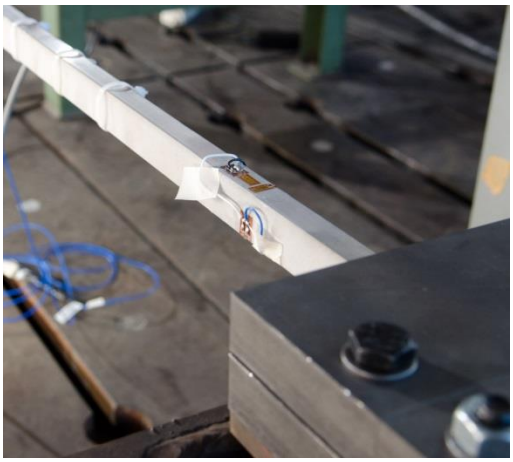

Fig. 5-4: the strain gauge

Sensitivity (±10 %)	Measurement Range	Frequency Range (±5 %)	Weight	Spectral noise (100Hz)
10.2 mV/(m/s²)	±490 m/s² pk	0.5 to 3000 Hz	4.0 g	33 (μm/s²)/√Hz

Table 5-2: accelerometer product specifications

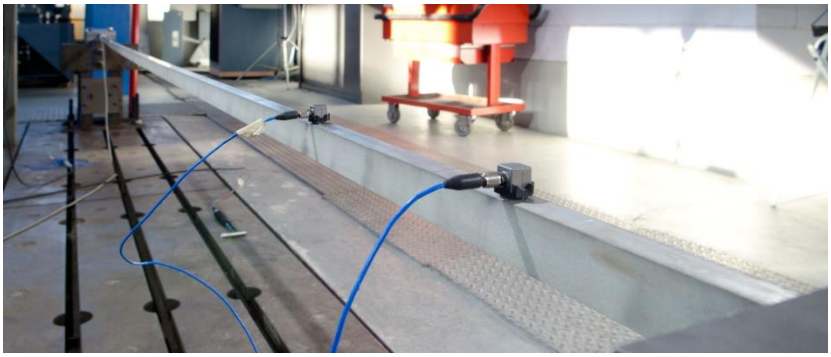

Fig. 5-5: accelerometers place at 3.5% and 9.5 % of the beam length

In addition to the bias introduced between the nominal length assigned to the FE model and the actual span on the test rig, the bias on the actual length participating to the mode shape of the tie-rod is affected also by other factors: the possibility to partially change the tightening of the clamps and the introduction of rubber layers between the constraints elements and the beam.

The basements where the constraint are fixed were design in order to avoid any static subsidence when the beam is tensioned as well as aiming to avoid dynamic effects on the mode shapes of the tie-rod. An FE model of the basement helped to investigate such an issue. Dynamic measurements are carried out for testing the dynamic behaviour of the basement. The numerical simulation and the experimental tests showed the effectiveness of the basement design in avoiding any issues.

The next section presents the results about the experimental tests carried out to provide an experimental validation of the method already numerically testes in Chapter 4. A lot of cases are tested, in terms of real axial load applied and constraint conditions (i.e. changing the tightening of the clamp as well as by interposing some rubber layers between them). In addition to the biases and uncertainties abovementioned about the actual beam span, the position where the accelerometers are placed are changed in order to simulate further biases on the length.

5.3 Experimental results

The results of the experimental are show for two different condition of constraints stiffness: adding or removing sheets of rubber between the rod and the plates closing it at its ends.

Fig. 5-6 shows the results achieved for tests measuring the input force (i.e. provided with an impact hammer) and performing experimental modal analysis, while Fig. 5-6 presents the results obtained with environmental excitation and operational modal analysis. The response of the beam was measured at $y1$ and $y2$ (see Section 2.4.2), calculated on the nominal length of 4000 mm. The maximum discrepancy (after updating) on load estimation was a little higher than 6%, in strict accordance with the simulations of Section 4.3. The results in terms of N, k, l, E and ρ are shown in Table 5-3 (without rubber sheets) Table 5-4 (with rubber sheet)

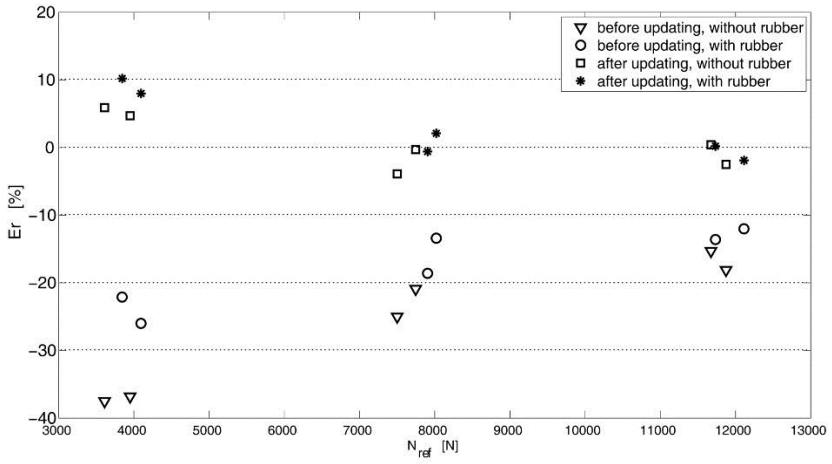

Fig. 5-6: experimental test results measuring the input force

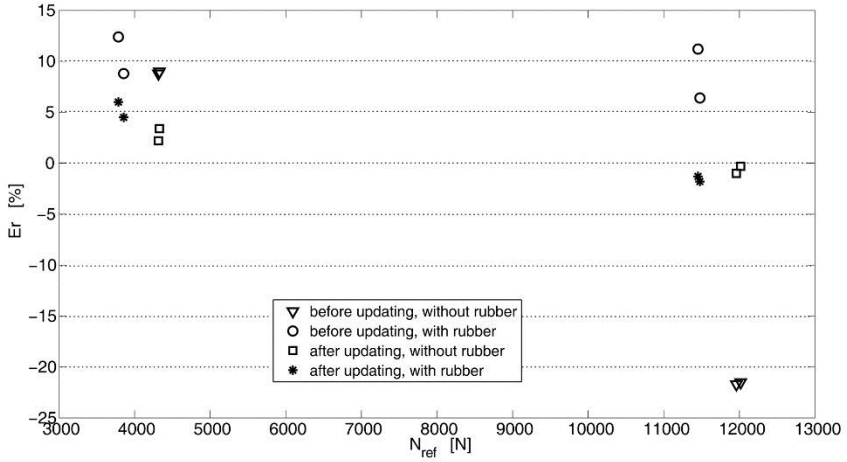

Fig. 5-7: experimental test results with environmental excitation

Parameter	**Tests without rubber sheets**					
N_{ref} [N]	3594	3949	7408	7746	11912	11673
N_{est} before upd.[N]	4029	4300	7650	8157	12115	12150
Er before upd. [%]	12,1	8,9	3,3	5,3	1,7	4,1
N_{est} after upd. [N]	3778	4139	7246	7602	11235	11395
***Er* after upd. [%]**	**5,1**	**4,8**	**-2,2**	**-1,9**	**-5,7**	**-2,4**
k_{est} before upd.	265	212	193	146	170	123
k_{est} after upd.	352	219	215	184	202	137
l nominal [mm]	4000	4000	4000	4000	4000	4000
l after upd. [mm]	3970	3995	3974	3963	3960	3970
E nominal [MPa]	68670	68670	68670	68670	68670	68670
E after upd. [MPa]	66979	68553	68046	65379	67540	66549
ρ nominal [kg/m^3]	2,69x10^{-9}	2,69x10^{-9}	2,69x10^{-9}	2,69x10^{-9}	2,69x10^{-9}	2,69x10^{-9}
ρ after upd. [kg/m^3]	2,69x10^{-9}	2,68x10^{-9}	2,69x10^{-9}	2,64x10^{-9}	2,65x10^{-9}	2,64x10^{-9}

Table 5-3: Results of experimental tests measuring the input force to the beam (without rubber)

Parameter	**Tests with rubber sheets**					
N_{ref} [N]	3844	4095	8021	7905	12113	11733
N_{est} before upd.[N]	4711	4759	8882	8375	12841	12310
Er before upd. [%]	22,5	16,2	10,7	5,9	6,0	4,9
N_{est} after upd. [N]	4095	4308	8061	7754	11859	11520
***Er* after upd. [%]**	**6,5**	**5,2**	**0,5**	**-1,9**	**-2,1**	**-1,8**
k_{est} before upd.	41	45	35	44	34	41
k_{est} after upd.	48	49	36	48	34	46
l nominal [mm]	4000	4000	4000	4000	4000	4000
l after upd. [mm]	3961	3960	3962	3962	3960	3974
E nominal [MPa]	68670	68670	68670	68670	68670	68670
E after upd. [MPa]	65989	65625	67276	65805	67366	67289
ρ nominal [kg/m^3]	2,69x10^{-9}	2,69x10^{-9}	2,69x10^{-9}	2,69x10^{-9}	2,69x10^{-9}	2,69x10^{-9}
ρ after upd. [kg/m^3]	2,64x10^{-9}	2,64x10^{-9}	2,64x10^{-9}	2,64x10^{-9}	2,64x10^{-9}	2,65x10^{-9}

Table 5-4: Results of experimental tests measuring the input force to the beam (with rubber)

Table 5-5 and Table 5-6 presents the results obtained with environmental excitation and operational modal analysis, respectively without and with the rubber sheets.

Parameter	**Tests without rubber sheets**			
N_{ref} [N]	4328	4315	12017	11960
N_{est} before upd.[N]	4716	4693	9438	9363
Er before upd. [%]	9,0	8,8	-21,5	-21,7
N_{est} after upd. [N]	4474	4411	11980	11838
***Er* after upd. [%]**	**3,4**	**2,2**	**-0,3**	**-1,0**
k_{est} before upd.	133	129	130	123
k_{est} after upd.	150	150	129	128
l nominal [mm]	4000	4000	4000	4000
l after upd. [mm]	3977	3981	3960	3965
E nominal [MPa]	68670	68670	68670	68670
E after upd. [MPa]	68068	68105	72103	72099
ρ nominal [kg/m^3]	2,69x10^{-9}	2,69x10^{-9}	2,69x10^{-9}	2,69x10^{-9}
ρ after upd. [kg/m^3]	2,70x10^{-9}	2,70x10^{-9}	2,64x10^{-9}	2,65x10^{-9}

Table 5-5: Results of experimental tests without measuring the input force to the beam (without rubber)

Parameter	**Tests with rubber sheets**			
N_{ref} [N]	3785	3855	11477	11452
N_{est} before upd.[N]	4255	4194	12213	12729
Er before upd. [%]	12,4	8,8	6,4	11,2
N_{est} after upd. [N]	4013	4029	11274	11299
***Er* after upd. [%]**	**6,0**	**4,5**	**-1,8**	**-1,3**
k_{est} before upd.	64	65	30	27
k_{est} after upd.	65	68	27	28
l nominal [mm]	4000	4000	4000	4000
l after upd. [mm]	3964	3966	3960	3965
E nominal [MPa]	68670	68670	68670	68670
E after upd. [MPa]	65357	65530	68254	68235
ρ nominal [kg/m^3]	2,69x10^{-9}	2,69x10^{-9}	2,69x10^{-9}	2,69x10^{-9}
ρ after upd. [kg/m^3]	2,68x10^{-9}	2,68x10^{-9}	2,64x10^{-9}	2,64x10^{-9}

Table 5-6: Results of experimental tests without measuring the input force to the beam (with rubber)

The maximum discrepancy (after updating) on load estimation was a little higher than 6%, in strict accordance with the simulations of Chapter 4.. The estimated k values are close among the same kind of tests with rubber sheets. The slight differences in its estimated values are also due to the varying torque applied to bolts closing the tie-rod at its ends (in fact, the mounting procedure was repeated for every test in order to fully check the method every time). As for tests without rubber sheets, the estimated values of k are not so close. Nevertheless, one should consider that a k equal to 100 or 300 makes a very slight difference under a physical point of view. In fact, both values indicate a situation very close to a perfect clamped-clamped condition, which shows that the eigenfrequency values tend not to change for a value of k higher than 100. As for the estimation of N before the updating, it tends to be positive since the length of the beam in the FE model is higher than the actual measured value.

Then, another kind of tests was carried out with experimental modal analysis. This time the position of the two accelerometers was again wrong on purpose but the bias was much higher than before. The length l was underestimated of 160 mm (i.e. l=3996-160 mm=3836 mm) and y1 and y2 were calculated as the 9.5% and 3.5% (see Section 2.4.2) of the fixed wrong length.

shows the results and again the method proved to work properly.

Parameter	**Tests without rubber sheets**			
N_{ref} [N]	3610	3949	7501	7746
N_{est} before upd.[N]	2255	2497	5629	6127
Er before upd. [%]	-37,5	-36,8	-25,0	-20,9
N_{est} after upd. [N]	3822	4133	7212	7724
***Er* after upd. [%]**	**5,9**	**4,7**	**-3,9**	**-0,3**
k_{est} before upd.	257	215	199	148
k_{est} after upd.	309	278	270	157
l nominal [mm]	3840	3840	3840	3840
l after upd. [mm]	3981	4013	3979	3980
E nominal [MPa]	68670	68670	68670	68670
E after upd. [MPa]	67386	69385	67209	68086
ρ nominal [kg/m^3]	2,69x10^{-9}	2,69x10^{-9}	2,69x10^{-9}	2,69x10^{-9}
ρ after upd. [kg/m^3]	2,67x10^{-9}	2,67x10^{-9}	2,67x10^{-9}	2,67x10^{-9}

Table 5-7: Results of experimental tests with high bias on l (without rubber sheets)

Parameter	**Tests with rubber sheets**			
N_{ref} [N]	3844	4095	8021	7905
N_{est} before upd.[N]	2995	3028	6944	6432
Er before upd. [%]	-22,1	-26,0	-13,4	-18,6
N_{est} after upd. [N]	4235	4420	8191	7856
***Er* after upd. [%]**	**10,2**	**8,0**	**2,1**	**-0,6**
k_{est} before upd.	42	46	35	45
k_{est} after upd.	42	46	35	45
l nominal [mm]	3840	3840	3840	3840
l after upd. [mm]	3972	3973	3969	3977
E nominal [MPa]	68670	68670	68670	68670
E after upd. [MPa]	68335	67619	68636	68495
ρ nominal [kg/m^3]	2,69x10^{-9}	2,69x10^{-9}	2,69x10^{-9}	2,69x10^{-9}
ρ after upd. [kg/m^3]	2,67x10^{-9}	2,67x10^{-9}	2,67x10^{-9}	2,67x10^{-9}

Table 5-8: Results of experimental tests with high bias on l (with rubber sheets)

Comparing the ith column of Table 16 and 17 with the ith column of Table 5-7 and Table 5-8, it is possible to have a more reliable check on the results achieved in terms of k. In fact, the torque of bolts was strictly the same for those tests and the estimated k values are very close each other. Furthermore, the value of l is always changed

correctly (i.e. increasing or decreasing from the nominal value, depending on the case) by the updating procedure.

The differences between the value of N estimated by the method and that measured by the Wheatstone bridge are of the same order of those achieved with other methods in literature (e.g. [12]).

CHAPTER 6

Assessment of the beam length

6.1 Introduction

The previous sections showed that it is possible to converge to a proper axial load estimation as soon as the range chosen for the l parameter in the updating procedure is within the 5 % of the actual length. This is of course a reasonable and acceptable threshold in many practical situations. Nonetheless, cases exist where the ends of the beam can be hidden and it is difficult to have an estimation of l.

This section aims to explain how to get a first estimation of the beam length. The target is to recognise when the discrepancy between the tie-rod actual length and the length of the visible portion is higher than 5 %.

The method presented here takes advantage of the considerations on the CoMAC method presented in Section 2.4. The value of this index showed to be sensitive to the features of the tie-rod. This sensitivity is now employed to find an estimate of the length of the beam. The next subsection explains the developed method.

6.2 Method to assess the beam length

Suppose to have a beam with a visible portion l_v lower than the actual value of l (Fig. 6-1). A reference FE model can be implemented. Such a model is characterised by nominal values of E, ν, N (i.e. a null load is fixed) and k (i.e. the model has k=∞, which turns into having a clamped-clamped beam) and l (i.e. l_v, which is the visible length). The FE model is presented in Fig. 6-1. A cross-correlation between the actual beam and the FE model implemented by means of the CoMAC index is able to give an assessment of the actual value of l. This is demonstrated by carrying out simulations using a further FE model which simulates the actual beam.

Relying on Fig. 6-1, the CoMAC index between the points of the actual beam and a single point of the FE model (Fig. 6-1) is able to indicate the value of l. The point chosen to use within the clamped-clamped FE model is at 20 % of lv. This choice depends on the fact that the point at 20 % already showed peculiar features (Section 2.4). Nonetheless, different points could be used as well.

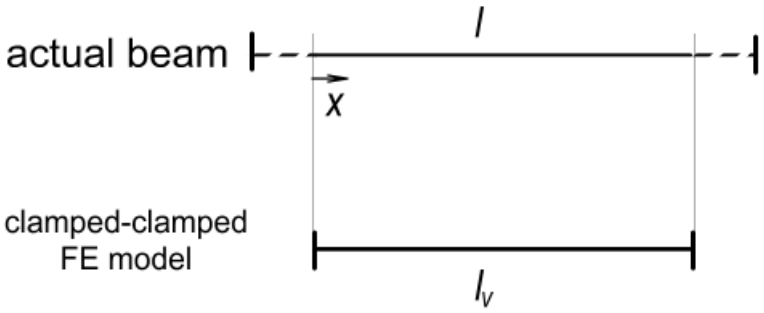

Fig. 6-1: Actual beam and its clamped-clamped FE model

If a curve relating the points of the actual beam (in the visible portion: see the coordinate x in Fig. 6-1) to the corresponding CoMAC values is plotted, it results to have a single maximum (Fig. 6-2). This maximum shifts in dependence of the value of l (Fig. 6-2). Therefore, the following procedure can be employed in a real application:

1. build a clamped-clamped FE model (see above for its features). This model is named Model C;

2. build another FE model, which simulates the actual beam with nominal data for E and ν. N is fixed to $N_{YL}/2$ and k to a middle value (e.g. 30). l is changed step by step, from l_v on. This model is named Model D;

3. the CoMAC between the points of Model D (in the visible portion) and the point at 20 % of l_v of Model C is calculated. The maximum of the resulting curve and its corresponding point in model D are computed for each value of l in model D;

4. a plot relating the position of the maximum in Model D and the actual value of l is achieved;

5. a modal identification on the real beam is carried out and the modal constants (scaled to the unit modal mass) are computed;

6. the modal constants are used to calculated the CoMAC with respect to the point at 20 % of l_v of Model C and the position giving the maximum of the CoMAC is found;

7. the knowledge of this position is cross-correlated with the curve achieved with models C and D (point 4 of this numbered list) and an estimated of l is found (i.e. lest).

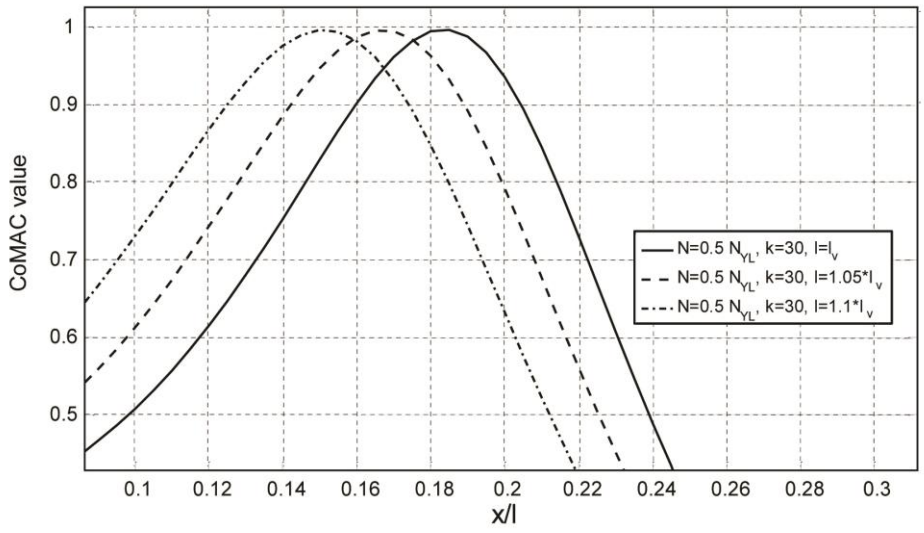

Fig. 6-2: Curves linking the position of the points on the actual beam to the corresponding CoMAC value

There is an issue not considered in the mentioned list. The Model D used to build the reference curve is characterised by nominal values but the actual beam could have different values for E, ν, N and k. Changes of these four variables can cause shifts of the maximum of the reference curve. The sensitivity of the position of the maximum of the CoMAC with respect to these variables is much less than that on l but it cannot be neglected. Thus, the uncertainty on these four variables must be taken into account. This is possible by repeating points 1 to 4 of the above procedure with extreme values

for E, ν, N and k in Model D. This allows to find an interval of possible values of l around lest.

Numerical simulations showed that the use of the modes from 1 to 6 to calculate the CoMAC allows to reach interval around lest of about 5 % of l (i.e. ±2.5 % or an interval with an equal width but non-symmetric, depending on the considered test case) in the worst case (slender beams made up of aluminium alloys). This width was reached by using not all the points of Model D to calculate the CoMAC but considering a resolution of 2 cm. The width of this interval can be lowered using lower resolutions (e.g. 5 mm) or using higher modes (e.g. modes from 6 to 8). Table 6-1 the results achieved with the test set-up shown in Section 5.2 (the actual length of the beam was 3996 mm).

The results are satisfactory and indicates that it possible to recognise if l is higher than $1.05 \times l_v$ and, in that case, to have an assessment of l.

	Without rubber sheets		With rubber sheets	
Test case 1	N/Nsn=0.3	N/Nsn=0.52	N/Nsn=0.26	N/Nsn=0.56
l_v [mm]	3796.0	3796.0	3796.0	3796.0
l_{est} [mm]	3974.5	3974.5	3984.1	4049.2
Error %	-0.539	-0.539	-0.298	1.332

	Without rubber sheets		With rubber sheets	
Test case 2	N/Nsn=0.3	N/Nsn=0.52	N/Nsn=0.26	N/Nsn=0.56
l_v [mm]	3596.0	3596.0	3596.0	3596.0
l_{est} [mm]	4007.2	4019.8	4022.1	4022.1
Error %	0.281	0.596	0.653	0.653

Table 6-1: Results of the experimental tests where the actual length of the beam was 3996 mm

CHAPTER 7

Conclusion

This thesis has dealt with the design, development and testing of an innovative technique to assess axial tensile load in tie-rods. These elements have a crucial role in structures since they assure their stability. Therefore, the monitoring of their status is of primary importance and different works were proposed in literature in the last years to assess the axial load they are subject to. Indeed, no methods exist allowing a direct measurement of the axial load, unless strain gages are bonded to the tie-rods before they undergo the operating conditions. Nonetheless, this is usually not possible, especially in ancient constructions. Then, indirect methods to estimate the axial load become the only possible solution.

Among the proposed methods, the dynamic techniques show some significant features, especially related to the ease of implementation, cost effectiveness and speed of tests. A number of works were presented in this decade and all of them study the modal features of the beam under analysis to get an estimation of the axial tensile load.

Although these techniques have very nice properties, all of them show some drawbacks: some of them require to have constant section of the beam along its length, other pose very strict conditions about the knowledge of the material properties, other did not undergo an experimental validation.

Therefore, there is still room for improvements and this work tries to fill some of the aforementioned gaps. The method designed and developed here is a dynamic approach and thus takes into consideration the modal behavior of the beam to analyse.

The goal of the work was to develop a method able to provide an accurate assessment of the axial load which results easy to apply both numerically and experimentally, without the need of knowing with a very low uncertainty the features of the tie-rod material. Furthermore, the method was expected to properly work with any kind of tie-rods, without requiring to have a constant section. This means that for example beams with screwed coupling joints could be considered as well. Finally, the method was expected to work even with environmental forcing (i.e. without measuring the input to the beam) in order to allow a continuous monitoring and thus cost-effective maintenance strategies.

The work started by studying analytical models in literature describing the dynamics of axially loaded beams. This task allowed to find which variables are able to affect the modal parameters of such structures. Then, finite element simulations were carried out to find which of them have significant influence of the dynamics of the tie-rods and get quantitative information.

The comprehension of the basic effects of geometrical and mechanical variables on the modal behavior of a beam was the starting point to design the new method to assess the axial load. The eigenfrequencies of the beam were found to be suitable to estimate the axial load but the analyses also showed that an estimation of the stiffness of the constraints was necessary prior to any other task. Hence, methods to assess the stiffness of the constraints were investigated and two approaches were proposed, both relying on the mode shapes of the beam.

The whole developed technique requires to cross-correlate the experimentally identified modal parameters with finite element models and such a task is able to lead to a first estimation of the axial load. Nevertheless, the numerical analyses also showed that the uncertainty affecting the other variables of the problem (e.g. the actual length of the beam and its Young's modulus) must be taken into account in order to have a reliable assessment of the axial load. The final estimation of the axial load is thus reached by a model updating procedure, which reasonably changes the features of the numerical finite element model according to the collected experimental data and leads to final estimation of the axial force.

Montecarlo simulations were thus performed in order to check the reliability of the designed method and to understand the level of confidence of the achieved results. The results showed that this new method is able to guarantee an accuracy close (or even

better in some cases) to that associated to the best methods in literature with less constraints (e.g. the necessity to know the Young's modulus of the material with a very high accuracy).

Finally an experimental validation of the method was carried out and the results confirmed those coming from the Montecarlo simulations.

The last part of the work develops an extension of the identification procedure, which allows to find a first estimate of the actual length of the beam. Indeed, this is an important information for the success of the model updating procedure when the actual length of the tie-rod is very different from the first trial value (i.e. the measurement of the visible portion of the beam).

Therefore, the designed method reaches all the goals fixed at the beginning of the work and it is noticed that the developed procedure does not require to measure the input to the structure. Furthermore, the number of sensors required to measure the response of the beam is limited to two. This makes the current method much cheaper with respect to most of the referenced techniques, even enabling to carry out continuous monitoring of the tie-rods.

References

[1] E. Giuriani, A. Marini, C. Porteri e M. Preti, "Seismic Vulnerability for Churches in Association with Transverse Arch Rocking", *International Journal of Architectural Heritage,* n. 3, pp. 212-234, 2009.

[2] S. Briccoli Bati e U. Tonietti, "Experimental methods for estimating in situ tensile force in tie-rods", *Journal of Engineering Mechanics,* n. 127, pp. 1275-1283, 2001.

[3] N. Tullini e F. Laudiero, "Dynamic identification of beam axial loads using one flexural mode shape", *Journal of Sound and Vivration,* n. 318, pp. 131-147, 2008.

[4] N. Tullini, "Bending tests to estimate the axial force in slender beams with unknown boundary conditions", *Mechanics Research Communications,* n. 53, pp. 15-23, 2013.

[5] T. Livingston, J. G. Béliveau e D. R. Huston, "Estimation of axial load in prismatic members using flexural vibrations", *Journual of Sound and Vivrations,* n. 179, pp. 899-908, 1995.

[6] S. Lagomarsino e C. Calderini, "The dynamical identification of the tensile force in ancient tie-rods", *Engineering Structures,* n. 27, pp. 846-856, 2005.

[7] M. Amabili, S. Carra, L. Collini, R. Garziera e A. Panno, "Estimation of tensile force in tie-rods using a fequency-based identification method", *Journal of Sound and Vibration,* n. 329, pp. 2057-2067, 2010.

[8] R. Garziera, M. Amabili e L. Collini, "A hybrid method for nondestructive evaluation of the axial load in structural tie-rods", *Nondestructive Testing and Evaluation,* vol. 26, n. 2, pp. 197-208, 2011.

[9] C. Gentilini, A. Marzani e M. Mazzotti, "Nondestructive characterization of tie-rods by means od dynamic testing, added masses and genetic algorithms", *Journal of Sound and Vibration,* n. 332, pp. 76-101, 2013.

[10] S. Li, E. Reynders, K. Maes e G. De Roeck, "Vibration-based estimation of axial force for a beam member with uncertain boundary conditions", *Journal of Sound and Vibration,* n. 332, pp. 795-806, 2013.

[11] G. Rebecchi, N. Tullini e F. Laudiero, "Estimate of the axial force in slender beams with unknown boundary conditions using one flexural mode shape", *Journal of Sound and Vibration,* n. 332, pp. 4122-4135, 2013.

[12] K. Maes, J. Peeters, E. Reynders, G. Lombaert e G. De Roeck, "Identification of axial forces in beam members by local vibration measurements", *Journal of Sound and Vibration,* n. 332, pp. 5417-5432, 2013.

[13] C. Blasi e S. Sorace, "Determining the Axial Force in Metallic Rods", *Structural Engineering International,* vol. 4, n. 4, pp. 241-246, 1994.

[14] S. Sorace, "Parameter models for estimating in-situ tensile force in tie-rods" *Journal of Engineering Mechanics,* n. 122, pp. 818-825, 1996.

[15] P. D. Greening e N. A. Lieven, "Identification and updating of loading in frameworks using dynamic measurements", *Journal of Sound and Vibration,* vol. 1, n. 260, pp. 101-115, 2003.

[16] A. S. Bahra e P. D. Greening, "Identifying axial load patterns using space frame FEMs and measured vibration data ", *Mechanical Systems and Signal Processing,* n. 4, pp. 1282-1297, 2009.

[17] A. S. Bahra e P. D. Greening, "Identifying multiple axial load patterns using measured vibration data ", *Journal of Sound and Vibration,* vol. 15, n. 330, pp. 3591-3605, 2011.

[18] S. P. Timoshenko e J. M. Gere, "Theory of Elastic Stability", New York: McGraw-Hill, 1961.

[19] L. Meirovitch, "Fundamentals of Vibrations", McGraw-Hill, 1996.

[20] H. T. M. Luong, L. F. Ramos e F. Aguilar, "Identification of the tensile force in tie-rods of historical constructions", in *XXIX International Conference on Modal Analysis pp 71-81*, Jacksonville, Florida, 2011.

[21] D. J. Ewins, "Modal testing: theory and practice", Research Studies Press, 2000.

[22] P. Trail-Nash e A. R. Collar, "The effects of shear flexibility and rotary inertia on the bending vibrations of beams", *Quarterly Journal of Mechanics and Applied Mathematics,* vol. 6, n. 2, pp. 186-222, 1953.

[23] J. W. S. Rayleigh, "The Theory of Sound", New York: Dover Publications Inc., 2003.

[24] S. P. Timoshenko, "On the correction for shear of the differential equation for transverse vibrations of prismatic bars", *Philosophical Magazine Series 6,* vol. 41, n. 245, pp. 744-746, 1921.

[25] S. P. Timoshenko, "On the transverse vibrations of bars of uniform cross section", *Philosophical Magazine Series 6,* vol. 43, n. 253, pp. 125-131, 1922.

[26] Evaluation of measurement data - Supplement 1 to the “Guide to the expression of uncertainty in measurement” - Propagation of distributions using a Monte Carlo method - JCGM - Joint Committee for Guides in Metrology, 2008.

[27] Evaluation of measurement data - Guide to the expression of uncertainty in measurement - JCGM - Joint Committee for Guides in Metrology, 2008.

[28] N. Tullini, G. Rebecchi e F. Laudiero, "Bending tests to estimate the axial force in tie-rods", *Mechanics Research Communications,* n. 44, pp. 57-64, 2012.